Geochemistry Geophysics Geosystems G3
AN ELECTRONIC JOURNAL OF THE EARTH SCIENCES
Published by AGU and the Geochemical Society

Article
Volume 9, Number 3
21 March 2008
Q03Q08, doi:10.1029/2007GC001813
ISSN: 1525-2027

Biogeochemistry of iron in Australian dust: From eolian uplift to marine uptake

Doug S. Mackie
Department of Chemistry, University of Otago, P.O. Box 56, 9001 Dunedin, New Zealand (dmackie@alkali.otago.ac.nz)

Philip W. Boyd
NIWA Centre for Chemical and Physical Oceanography, Department of Chemistry, University of Otago, 9001 Dunedin, New Zealand

Grant H. McTainsh
Griffith School of Environment, Australian Rivers Institute, Griffith University, Brisbane, Queensland 4111, Australia

Neil W. Tindale
Faculty of Science, Health and Education, University of the Sunshine Coast, Maroochydore DC, Queensland 4558, Australia

Toby K. Westberry
Department of Botany and Plant Pathology, Oregon State University, Corvallis, Oregon 97331-2902, USA

Keith A. Hunter
Department of Chemistry, University of Otago, P.O. Box 56, 9001 Dunedin, New Zealand

[1] Dust is an important vector for iron supply to the ocean, which subsequently impacts ocean productivity, atmospheric CO_2 concentrations, and hence global climate. Here, we synthesize the processes influencing the biogeochemistry of Australian dust and compare them with those from other Southern Hemisphere dust sources. Our observations range from soil and dust physical properties to abrasion and cloud chamber chemistry experiments to dust storms and their dispersion and deposition. We then present satellite observations of the impact of episodic dust deposition events on the productivity of low-iron oceanic waters north (i.e., low-nitrate, low-chlorophyll (LNLC)) and south (i.e., high-nitrate, low-chlorophyll (HNLC)) of Australia. Dust deposition from the largest dust storm in over 40 years did not result in iron-mediated algal blooms in either oceanic region. A comparison of Australia with other Southern Hemisphere source regions reveals that the relatively well sampled Australian system is a poor generic model. Furthermore, there are marked distinctions between Southern and Northern Hemisphere iron/dust biogeochemistry that must be recognized by modelers and included in future simulations. Better information is required on the relative role of the atmosphere and ocean on influencing iron biogeochemistry and how their relative influences might change in the future due to climate change.

Components: 16,503 words, 11 figures, 3 tables.

Keywords: eolian dust; iron; biogeochemistry; phytoplankton; dissolution.

Index Terms: 0305 Atmospheric Composition and Structure: Aerosols and particles (0345, 4801, 4906); 0414 Biogeosciences: Biogeochemical cycles, processes, and modeling (0412, 0793, 1615, 4805, 4912); 0480 Biogeosciences: Remote sensing.

Received 4 September 2007; **Revised** 22 November 2007; **Accepted** 1 February 2008; **Published** 21 March 2008.

Mackie, D. S., P. W. Boyd, G. H. McTainsh, N. W. Tindale, T. K. Westberry, and K. A. Hunter (2008), Biogeochemistry of iron in Australian dust: From eolian uplift to marine uptake, *Geochem. Geophys. Geosyst.*, *9*, Q03Q08, doi:10.1029/2007GC001813.

1. Introduction

[2] It has long been acknowledged that dust supply impacts global climate by altering atmospheric aerosol loading, specifically cloud condensation nuclei production and radiative forcing [*Jickells et al.*, 2005]. In the last two decades, it has emerged that dust can also impact global climate through its role as a major source of iron to the upper ocean via episodic dust storms [*Prospero*, 2002]. In several oceanic regions, including the high-nitrate, low-chlorophyll (HNLC) waters of the Southern Ocean, mesoscale perturbation experiments have demonstrated that low iron availability limits primary production [*Boyd et al.*, 2007], and shipboard experiments in some oligotrophic (low-nitrate, low-chlorophyll, LNLC) tropical and subtropical areas indicate that low iron supply results in low N_2 fixation [*Mills et al.*, 2004] by diazotrophic phytoplankton.

[3] It has been proposed that increased iron supply in the geological past, specifically the glacial maxima [*Martin et al.*, 1990], resulted from higher dust fluxes [*Calvo et al.*, 2004]. This greater iron supply was probably responsible for higher rates of both primary production and carbon sequestration to the oceans interior, with a subsequent impact on climate via a reduction in atmospheric CO_2 concentrations [*Martin et al.*, 1990]. Subsequent analysis of Antarctic ice cores has supported this hypothesis and shown that during the last 420,000 years the rate of dust deposition is inversely correlated to atmospheric concentration of CO_2 [*Petit et al.*, 1999], and during the Last Glacial Maximum (LGM; 22–19 ka) the flux of acid-leachable iron was 34 times higher than at the start of the Holocene [*Gaspari et al.*, 2006]. Other potential climatic impacts of dust-derived iron supply limiting the growth of marine phytoplankton include reduced production of albedo-enhancing aerosol precursors (e.g., dimethylsulfide) by phytoplankton [*Charlson et al.*, 1987; *Cropp et al.*, 2005].

[4] Early dust studies, such as SEAREX (SEA AiR EXchange Program; 1979–1987), focused on assessing the main regional sources, transport routes and seasonality of deposition of aerosol dust into the ocean [*Prospero et al.*, 1989]. A synthesis of these regional studies led to the first global maps of dust deposition into surface waters [*Duce and Tindale*, 1991]. Subsequent research using laboratory-based solubility experiments sought to translate these maps of dust deposition into global distributions of iron deposition [*Spokes et al.*, 1994]. Remote-sensing has become a powerful tool to provide large-scale monitoring of transport routes and deposition zones [*Husar et al.*, 1997] that has improved our understanding of the scale and episodicity of global dust processes.

[5] More recent research has focused on many aspects of dust processes including regional estimates of dust solubility [*Baker et al.*, 2006], the role of land use in altering dust supply [*Tegen et al.*, 1996], soil abrasion and dust particle size [*Bullard et al.*, 2004], and dust interactions with sunlight [*Tagliabue and Arrigo*, 2006] and cloud water [*Hand et al.*, 2004; *Mackie et al.*, 2005]. However, despite the increased scope of dust research, very few studies have attempted an overview of these processes (and how they interrelate), and many key areas remain un-addressed; *Jickells et al.* [2005], in a review of the connections between dust and ocean biogeochemistry and their impact on climate, recommended that future research needs to focus on areas such as dust deposition processes, and aerosol iron bioavailability.

[6] Observations of dust transport and deposition have been dominated by reports from the Northern Hemisphere (e.g., see summary tables of *Duce et al.* [1991]). Recent large scale dust-related programs such as ACE-Asia [*Chuang et al.*, 2005] and PRIDE [*Reid et al.*, 2003] have continued this trend by studying dust emissions and transport from China and the Sahara, respectively. Current global models of dust emission, transport and deposition predict that <20% of global oceanic dust deposition is into Southern Hemisphere waters and, that due to the relative proportions of land to water, dust deposition per m^2 to Northern Hemisphere oceans is 6–22-fold greater than to Southern Hemisphere waters (Table 1). However, the impact of dust supply on oceanic biota in a

Table 1. Relative Dust Emissions and Depositions to the Oceans of the Northern and Southern Hemispheres[a]

	Prospero [1996]	*Ginoux et al.* [2001]	*Zender et al.* [2003]	*Jickells et al.* [2005]
North Atlantic	220	184	178	202
North Pacific	96	92	31	72
North Indian	20	138	36	81[b]
N. oceans total	336	414	245	355
South Atlantic	5	20	29	17
South Pacific	8	28	8	29
South Indian	9	16	12	37[b]
S. oceans total	22	64	49	83
N% area	94	87	83	81
S% area	6	13	17	19
N. oceans, g m^{-2}	2.2	2.7	1.6	2.3
S. oceans, g m^{-2}	0.1	0.3	0.2	0.4

[a] Dust emissions and depositions are in Tg a^{-1}. Each of the models has used selected observational data from University of Miami stations [*Prospero*, 1996] to constrain outputs and this data is also included. No data is available for the Arctic Ocean and dust supply is assumed to be zero. Here, the Atlantic, Pacific and Indian oceans are taken as extending southward to the coast of Antarctica.
[b] Calculated from value for entire Indian Ocean, assuming the measured 20:9 proportion of *Prospero* [1996].

particular region is not necessarily a function of mass flux: "Although dust sources in the Southern Hemisphere are relatively small compared to those in the Northern Hemisphere, they warrant study because they could have a disproportionate impact on ocean productivity due to their proximity to the large HNLC (High Nitrate Low Chlorophyll) areas in the southern oceans" [*Mahowald et al.*, 2005, paragraph 50]. Factors influencing iron limitation are examined in section 3.

[7] Here, we focus attention on the role of iron and dust biogeochemistry in the Southern Hemisphere by bringing together recent data sets describing and linking the sequence of processes from the initial eolian uplift of Australian dust to the eventual uptake of dust-derived iron by phytoplankton in the waters offshore of Australia and New Zealand (Figure 1). By linking these processes, we can better identify gaps in our current knowledge of iron and dust biogeochemistry in this region, and cross-reference them to the future research priorities outlined by *Jickells et al.* [2005]. We then compare and contrast the characteristics of Australian dust processes with both other major Southern Hemisphere dust sources, and also with dust processes in the Northern Hemisphere. As this is a synthesis, methodological details are largely in the relevant papers and also briefly outlined in the relevant discussion.

2. Synthesis of Results/Findings

2.1. Australia as a Continental Dust Source

[8] A distinctive feature of Australian dust storm activity is its highly episodic nature. The major dust source regions in the northern Hemisphere; the Sahara and China, emit dust more continuously and in much greater quantities [*Washington et al.*, 2003]. This episodicity is largely because the Australian arid zone is relatively more humid, and better vegetated, than other arid regions. Also, being a very old continent with a complex geology has produced a complex matrix of soils with highly variable wind erodibility [*McTainsh et al.*, 1990].

[9] Spatial and temporal patterns of atmospheric dust entrainment in Australia have been measured using meteorological records in various ways. Initially the dust storm frequency was the measure of dust activity [*McTainsh and Pitblado*, 1987; *Middleton*, 1984]. This relationship was first quantified by *McTainsh et al.* [1989], who found a strong positive relationship between dust storm frequency and the number of meteorological stations recording dust activity. That is, during periods when dust storms are more frequent they are also cover larger continental areas. Dust storm frequency has been superseded by the Dust Storm Index (DSI) [*McTainsh*, 1998] which measures both the frequency and intensity of dust entrainment using records of dust events weighted according to the extent to which they reduce visibility.

[10] An improved version of the index (DSI_3) [*McTainsh et al.*, 2006] is used here to map dust activity (Appendix A and Figure 2). It is important to note that the DSI is descriptive and not predictive. The DSI has a very high correlation (r^2 0.98) against measured dust concentrations [*McTainsh et al.*, 2004]. While these maps of dust activity provide the best available measurements of dust

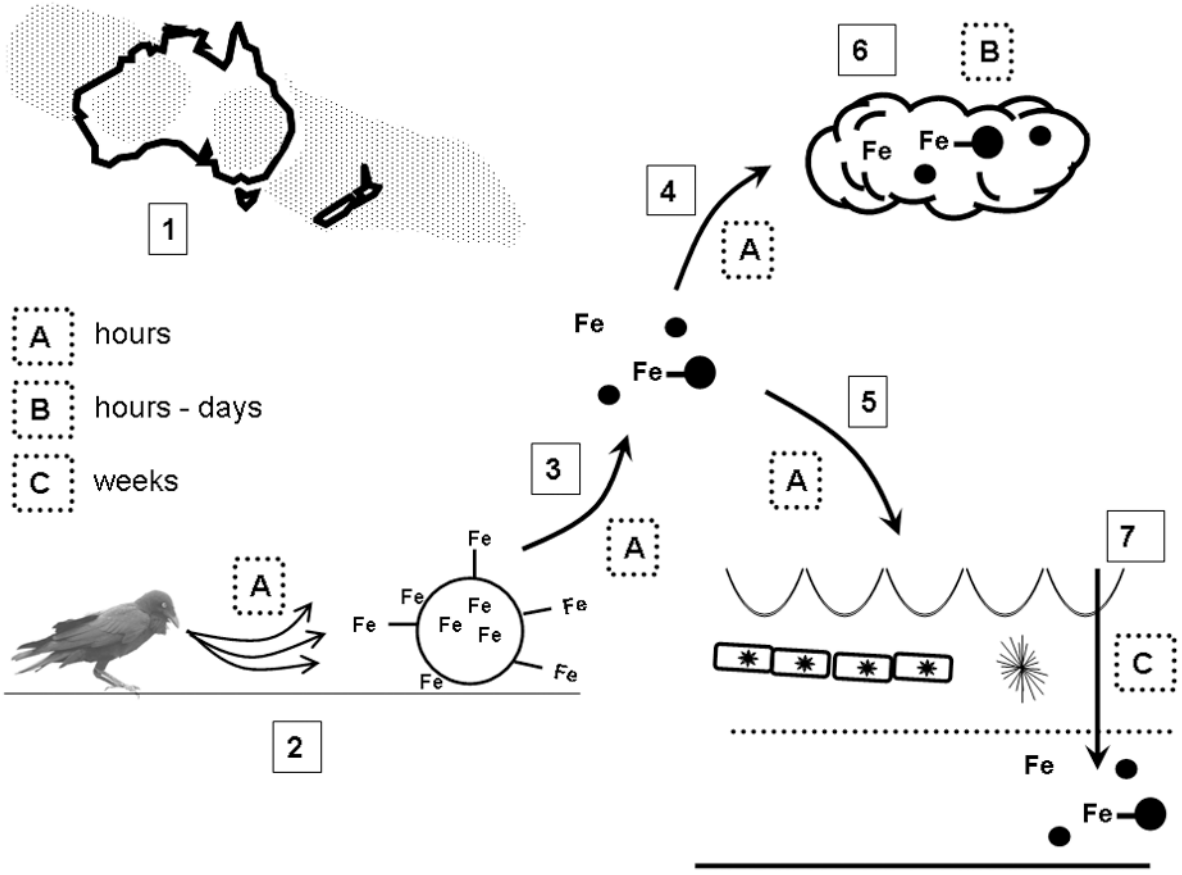

Figure 1. Schematic of the sequence and timescale of events from the uplift of Australian dust to the uptake of iron by biota: (1) Approximate dust pathways from Australia. (2) Winds (represented by the raven Bellin-Bellin, an aboriginal wind god from Victoria) uplift soil grains that have iron oxides bound to the surface and in loose association with the surface and iron compounds within the mineral matrix. (3) During uplift soils undergo abrasion, producing smaller grains by spalling, etc., and abrading iron-oxide coatings from grains. After abrasive uplift grains either are deposited directly into the ocean (5) or undergo further processing in the atmosphere, e.g., UV irradiation (4), acidic clouds (6), before oceanic deposition (7). In the ocean iron may be supplied to *Trichodesmium* cells (puffs) resident in LNLC subtropical waters north and east of Australia and New Zealand (NZ), and diatoms (chains) resident in HNLC waters south of NZ and Australia. Dusts have a residence time of weeks before passing from the mixed layer.

source areas (see below), their utility is limited by the small number of recording stations (Figure 2) and their sparse spatial distribution in the most dusty parts of the continent. Trained observers at 109 stations run by the Australian Bureau of Meteorology have provided continuous data since 1960 and approximately 100 additional stations have contributed observations at certain times. However, in recent times the number of full time professionally staffed stations has begun to decrease. *Leys et al.* [2006] are responding to this challenge by using a volunteer network, called DustWatch, to provide high spatial resolution dust monitoring.

[11] Most of the dust activity is in the centre of the continent (Figure 2), which reflects in part the inverse relationship between rainfall and dust entrainment [*Bullard and McTainsh*, 2003; *McTainsh et al.*, 1989]; however, the relationship is not a simple one. *McTainsh* [1985] and *Bullard and McTainsh* [2003] have concluded that the inland river systems of the Murray-Darling and Lake Eyre Basins (in the eastern sector of the continent) play an important role in feeding sediment into the arid centre where it is entrained into the atmosphere by strong wind events.

[12] The 46 year record of dust activity, measured by DSI_3 (Figure 3), shows three periods of high

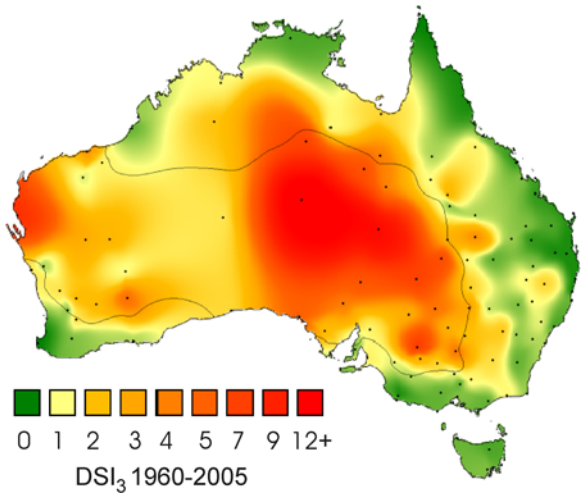

Figure 2. Annual mean DSI_3 for Australia, 1960–2005. The 400 mm isohyet indicated by solid black line. Black dots represent observing stations. Note that this is a smoothed temporal record because of intersectoral differences in rainfall and resultant dust activity between the west and eastern sectors of the continent which tend to cancel each other out. Generally speaking, when the east is in drought, the west is experiencing higher than average rainfall and vice versa.

dust activity; 1960–1972, 1994 and 2002–3, all of which are associated with droughts. Most recently, the onset of drought in 2002 resulted in a large increase in dust activity. The DSI for 2001 is 61 compared with 408 in 2002 (the highest DSI since records began in 1960). The DSI patterns for 2001 and 2002 (Figure 4) demonstrate how the location and extent of dust source areas can change dramatically in a short time.

[13] Within the large dust source regions there are a number of smaller dust source areas which become active at different times. A study of the relative erodibility of three land types, claypans (forming the high floodplains), dunes (linear, riverside dunes) and downs (interfluve areas between main rivers), in the Channel Country within the Lake Eyre Basin dust source region found that the erodibility of these land types changes considerably through time [*Butler et al.*, 2001; *McTainsh*, 1999]. The erodibility of the dunes and downs fluctuated significantly with annual rainfall because erosion on these land types was vegetation-limited, whereas on the alluvial claypans (the most erodible land type) the erosion rate was more constant because these saline surfaces were devoid of vegetation and therefore their erosion was influenced by soil surface erodibility.

[14] Large dust storms occur during periods of drought. For example, the 23 October 2002 dust storm (described by *McTainsh et al.* [2005] and *Shao et al.* [2007]) eroded 96 Tg of soil and entrained ~5 Tg dust along a 2,400 km front that swept across most the eastern seaboard of Australia (Figures 5a and 5b). During "average" (i.e., wetter) years dust storms are smaller and less frequent, and only the most erodible source areas are active. This produces a complex pattern of dust activity, which is evident in the 2001 DSI map (Figure 4).

[15] Remote-sensing-based studies tend to underestimate Australian dust emissions because most dust entrainment in this region results from meteorological cold fronts associated with cloud cover, which traps entrained dust at low elevations [*McGowan et al.*, 2005]. Simulations from global dust models in this region are, similarly, not without problems. For example results from *Ginoux et al.* [2001] compare their modeling simulations with measurements at Cape Grim (41°S 144°E) with some success. However, Cape Grim was originally established as a "pristine" site as most of the air is delivered by the predominant westerlies and few dust storm events pass due south over Tasmania from the source regions (Figure 6). Their results tend to overestimate early summer emissions and underestimate late summer emissions relative to ground-based measurements on mainland Australia [e.g., *Ekström et al.*, 2004; *McGowan et al.*, 2000; *McTainsh et al.*, 1989; *McTainsh and Pitblado*, 1987; *Raupach et al.*, 1994]. Other models overestimate the source strength of the Australian continent [e.g., *Bauer*

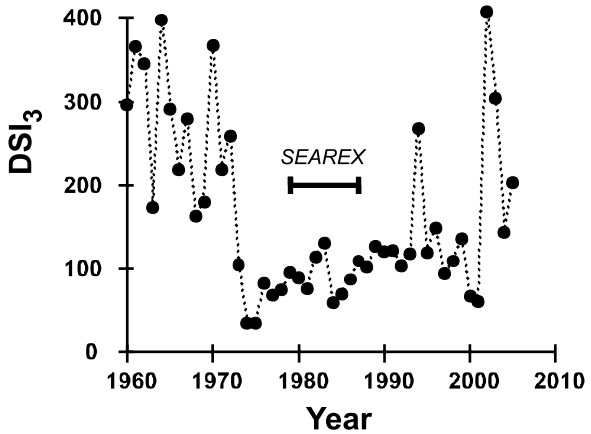

Figure 3. Temporal record of dust activity in Australia (1960–2005) measured by DSI_3. The time period covered by the SEAREX program is indicated and corresponded with low DSI_3 values.

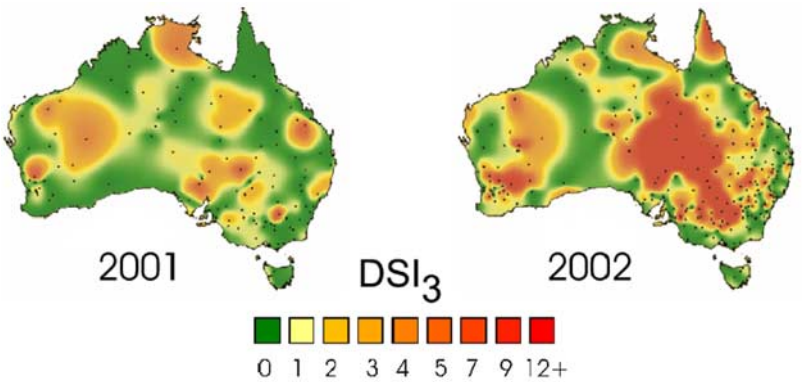

Figure 4. Contrasting spatial patterns of DSI_3 dust source areas in the consecutive years 2001 and 2002.

et al., 2004] and their outputs do not compare well with satellite records of dust transport [*Perlwitz et al.*, 2001]. These mismatches probably reflect both the location and quality of the validation data and assumptions made by the models. There is clearly a need for better high resolution information on dust sources, entrainment and transport processes, before significant advances can be made in our understanding of dust inputs to the ocean.

2.2. Dust Transport Pathways and Dust Loads

[16] There are two major dust paths passing offshore from Australia (Figure 6). The SE path moves across the SE landmass sector and passes over the Coral Sea, Tasman Sea and Southern Ocean while the NW path crosses the NW landmass and then over the Indian Ocean [*Bowler*, 1976]. Within each dust pathway, individual dust trajectories can be further identified, each with a distinct source region (described in terms of sectors of major drainage basins) and a particular seasonality. The NW dust path appears to be more directionally consistent, but this requires further confirmation as the pathway has received relatively little research effort. The SE dust path is examined in detail here, as it is the more active and appears to supply more dust to the Southern Ocean. Within the SE dust pathway, there are three dust trajectories with distinct source regions and seasonality [*McTainsh and Leys*, 1993] (1) NE over the Coral Sea (most active between September and December with a source region in the northern Lake Eyre Basin), (2) SE over the Tasman Sea (most active between December and March with a source region in the southeastern sector of the Lake Eyre Basin and the southern Murray-Darling basin) and (3) south over the Southern Ocean (most active between December and March with a source region in the southern sectors of the Lake Eyre and Murray-Darling Basins).

[17] Australian dust plumes can carry large sediment loads. During a single dust storm, lasting less than a day, in 1987 1.9–3.4 Tg of soil, ~30–50% of the estimated average annual dust export from Australia into the South Pacific, left the east coast of the Australian continent [*Knight et al.*, 1995]. The storm which engulfed Melbourne on 8 February 1983 carried 2 Tg of dust [*Raupach et al.*, 1994] and the largest recorded (since ~1960) event-based dust load (on 23 October 2002) was ~4.9 Tg [*McTainsh et al.*, 2005]. There are, however, significant technical difficulties associated with accurately measuring dust loads. For example, *McTainsh et al.* [2005] conclude that previous estimates of dust loads may be significant overestimates, because an assumption that dust concentration profiles are uniform with height is not always satisfied. Using the 23 October 2002 dust storm, *McTainsh et al.* [2005] showed that if a uniform concentration profile is assumed the calculated dust load would be 15.4 to 25.8 Tg, compared with their 3.4 to 4.9 Tg estimate, which assumes more realistically that dust concentration decreases with height according to the well-established power law [*Chepil and Woodruff*, 1957]. The numerical modeling of this dust storm by *Shao et al.* [2007] allows an approximate dust burden of ~5.1 t km^{-2} to be calculated; this is comparable with the 4.8 t km^{-2} dust load in a large dust storm in China (in April 2001) estimated by *Gu et al.* [2003]. Typical estimates for dust emissions from the Sahara are estimated at ~200 Tg per month [e.g., *Colarco et al.*, 2003a] and during the dustier winter months the Bodélé depression in northern Chad emits an average of ~0.7 Tg dust per day [*Koren et al.*, 2007].

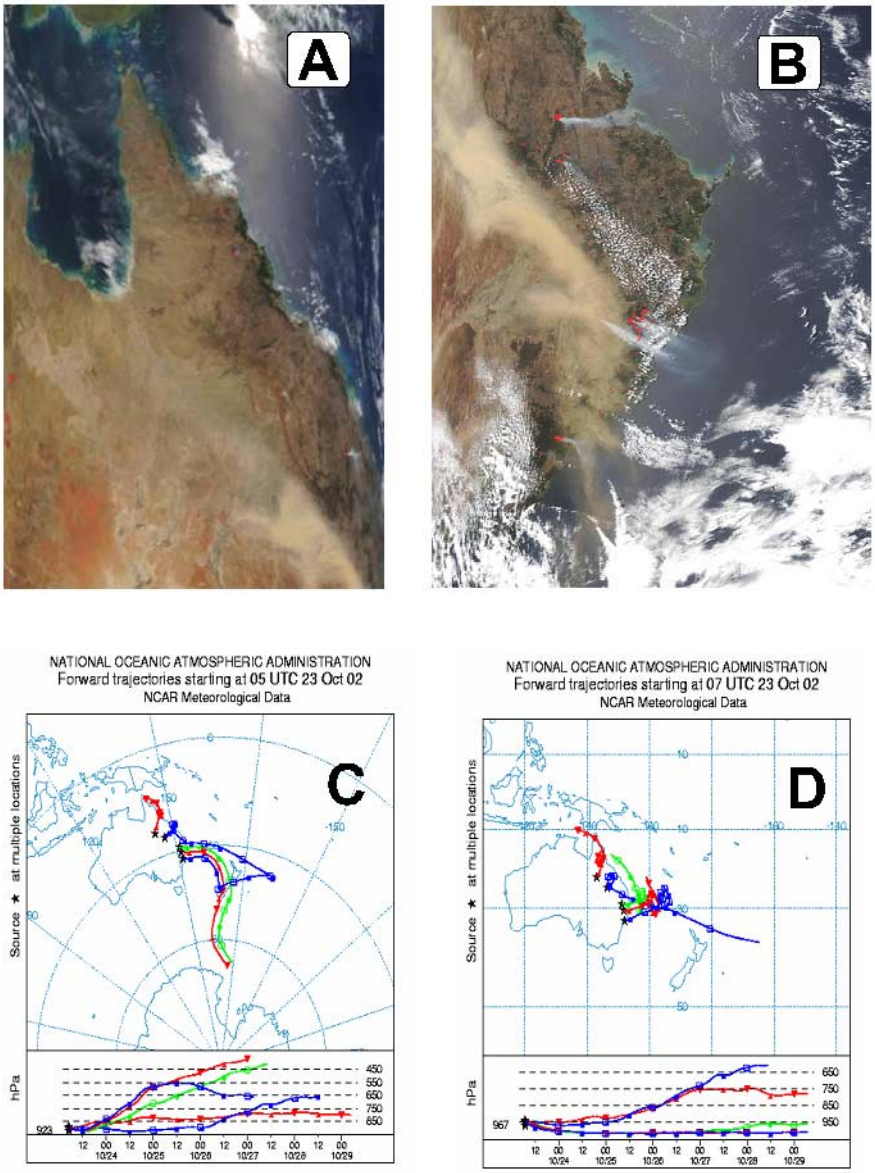

Figure 5. Dust event of 23 October 2002 over NE Australia and the Gulf of Carpentaria (see Figure 6) from (a) the MODIS Terra sensor (1005 h local time overpass) and (b) the MODIS Aqua sensor (1335 h local time overpass, with a more detailed view). The storm front is ~2400 km long. (c and d) Air mass back trajectories (from NOAA HYSPLIT) which illustrate the bifurcation of this dust plume as it moved offshore, moving both across Low Nitrate Low Chlorophyll (LNLC) waters north of Australia and NZ and over High Nitrate Low Chlorophyll (HNLC) waters south of NZ. Image courtesy of MODIS Rapid Response Project at NASA/GSFC. Details of the NOAA HYSPLIT model, 2003, are available at http://www.arl.noaa.gov/ready.html and are given by *Draxler and Hess* [2004].

2.3. Dispersion of Dust Plumes and Dust Deposition During Transport

[18] The fine (0.6–5 μm; clay/very fine silt) fraction of Saharan dust is transported within the distinctive Saharan Air Layer (SAL) [*Prospero and Carlson*, 1972]; an elevated layer of heated dry air from the Sahara above an inversion at 1.2 km to 1.8 km. However, the bulk of Saharan material that is deposited in the equatorial North Atlantic is transported by the NE trade winds. For the Southern Hemisphere there is little evidence of SAL like transport in the south east dust path, although *Healy* [1970] suggested that trans-Tasman dust transport could occur within a high altitude jet stream. Perhaps the most distinctive differences for dust transport into the Southern Ocean compared to

Figure 6. Map showing Australian dust transport pathways, modified after *Bowler* [1976] based upon new evidence on dust plume trajectories [*McGowan et al.*, 2000], and locations discussed in the text.

the North Atlantic is that southern transport of dust is impeded by the circumpolar westerlies, and probably only occurs during low points in this easterly airflow [*Delmonte et al.*, 2004a].

[19] Little is known about the vertical and lateral dispersion of Australian dust plumes following uplift [*McGowan et al.*, 2000]. Early research, in the Northern Hemisphere, into the relative contribution of lateral versus vertical dispersion [e.g., *Hamonou et al.*, 1999] was based on studies of the load distribution of both dust and pollution aerosols within dust clouds and layers, and used a range of approaches including satellite imagery, ground-based observations (e.g., sun-photometry), meteorological observations and air mass back-trajectory analysis. Much of the observed dispersion was evident as layers, and these reflect horizontal layering of the atmosphere and hence horizontal flow rather than vertical mixing [*Hamonou et al.*, 1999]. Space-borne LIDAR (Light Detection And Ranging) backscatter is a powerful way to look at vertical distributions of dust aerosols within plumes [*Berthier et al.*, 2006]. With the exception of some LIDAR studies based at Cape Grim, Tasmania (41°S) and on mainland Australia (Mildura, Victoria; 34°S) [*Boers et al.*, 1994; *Rosen et al.*, 2000] and some single particle and particle size studies, like the ACE-1 experiment at Cape Grim and south of Tasmania [*Bates et al.*, 1998], little research has been done in Australia to investigate dispersion.

[20] More recent studies in Australia have used remote-sensing to examine how dust plume dimensions during large storms can change on a timescale of days (such as the October 2002 event [*McTainsh et al.*, 2005]). Another potential tool to examine the lateral dispersion of a dust plume is the use of an offset in overpass times by MODIS (Moderate Resolution Imaging Spectroradiometer) Terra and Aqua satellite sensors (Figures 5a and 5b). *Boyd et al.* [2004] suggested that during a 3 d Australian dust event a horizontal dispersion factor of up to 8 might occur. This estimate is based on reports from *Gorden* [1986] that the horizontal dispersion parameter of a cloud in the boundary layer is ~50 km d^{-1}, and assuming a Gaussian profile, the radius of a circle containing 95% of the cloud changes at the rate of ~100 km d^{-1}.

[21] The deposition of dust during transport will be impacted by many factors including dust load, particle size, dust concentration profiles, dust ceilings, and downwind dust plume dispersion rates [*McTainsh*, 1999]. *Prospero et al.* [1989] reported a useful term for dust deposition: the "half-decrease" distance for a dust load (i.e., the distance over which ½ of the dust load is deposited). They calculated a range of half-decrease distances from 500 km (NW Pacific) to 2000 km (S Pacific). However, in the absence of regional data to estimate this term, assumptions for the ½ decrease distance for the Australasian region have to be made.

[22] Deposition of dust in the Australian region can be either wet (episodic and high rates of deposition) or dry (sustained, low rates of deposition), but few data on the proportion of wet:dry deposition are available. *Boyd et al.* [2004] have advocated that data on local rainfall patterns, from microwave and radar satellite sensors such as SSM/I (Special Sensor Microwave Imager) and TRMM (Tropical Rainfall Measuring Mission) combined with dust plume trajectories would be a useful way to distinguish between wet and dry deposition and provide much needed regional data on such processes.

2.4. Changes in Mineral Properties During Atmospheric Uplift and Dissolution of Iron From Dust by Cloud Processing

[23] Winds entrain dust into the lower atmosphere by simple uplift of existing dust deposits (formed in situ during previous wind events, or transported from elsewhere by previous wind and water events; section 2.2), or by uplift of dust produced in situ by abrasion processes (saltation, spalling and disaggregation) [*Grini and Zender*, 2004; *Leys et al.*, 1996; *Shao*, 2001]. During uplift and transport, dust is exposed to a range of environmental conditions that facilitate dissolution of iron. As discussed below, particle size influences the solubility of iron in mineral dusts [*Baker and Jickells*, 2006] and during abrasion processes the size of particle produced can vary markedly [*Bullard et al.*, 2007]. Furthermore, the particle size distribution after long-distance lateral transportation (e.g., Canary Islands to Puerto Rico) is not easily predicted [*Maring et al.*, 2003]. These considerations mean that it is currently convenient to simulate abrasion processes in laboratory experiments [*Bullard et al.*, 2007; *Mackie et al.*, 2006].

[24] During the simulated eolian abrasion of artificial dusts formed from soils taken from Australian source regions, the total amount of readily released iron remains unchanged but it is redistributed to smaller grains [*Mackie et al.*, 2006]. This suggests that the amount of readily released iron is an intrinsic property of a dust-source soil at the time of uplift. Subsequently, the amount of readily released iron may be set by the frequency of ground-based (as opposed to atmospheric) processing events (i.e., weathering and/or abrasion) since the dust or soil last experienced an uplift event.

[25] Large areas of SE Australia have soils in which a significant component of their dust has been gradually transported, possibly in a stepwise manner, from regions further west [*McTainsh*, 1999; *Ryan and Cattle*, 2006]. *Bullard and McTainsh* [2003] describe this stepwise dust transport, using a model of fluvial-eolian sediment cycling involving; the eastward-moving dusts and westward-flowing rivers of the Murray-Darling Basin. Thus, secondary source dusts in the Murray-Darling Basin that have undergone multiple uplift events, may be lower in readily released iron than some dusts from primary dust source regions like the Lake Eyre Basin.

[26] Laboratory-based studies suggest that, once uplifted, dust can undergo extensive atmospheric physico-chemical processing, especially in clouds [*Desboeufs et al.*, 2005; *Zhuang et al.*, 1992a], and often over several cycles of evaporation and hydration with associated pH changes, which enhance the dissolution of iron and other elements from the dust [*Mackie et al.*, 2005; *Spokes and Jickells*, 1996]. As a first approximation it has proved convenient to carry out laboratory experiments investigating dissolution of iron from mineral dusts under simple conditions using only strong mineral acids (i.e., in the absence of ligands, high energy photochemistry, or reducing agents) [*Desboeufs et al.*, 2005; *Mackie et al.*, 2005; *Spokes et al.*, 1994]. Such experiments offer an upper bound for the level of iron potentially available to oceanic phytoplankton via physico-chemical processes but it is important to note that in the presence of UV light, siderophores, and electron donors like oxalate the solubility of iron from dust is significantly increased [*Borer et al.*, 2005]. Sulfates, nitrates and carboxylic acids, especially oxalic acid, are common in aerosols and cloud waters with anthropogenic contamination and enhance the dissolution of mineral dusts [*Huang et al.*, 2006; *Matsuki et al.*, 2005; *Zuo and Zhan*, 2005]. However, in remote areas oxalic acid concentrations are typically 20–100 times lower than in urban air (10–50 ng m^{-3} compared to 900 ng m^{-3}) [*Warneck*, 2003] so organic compounds like oxalate may be less relevant to the more pristine air masses moving offshore from Australia.

[27] While the mineralogy of Saharan and Australian dusts is different [*Kiefert et al.*, 1996], the iron in Australian dust is similar to that of the Sahara [*Bonnet and Guieu*, 2004; *Spokes and Jickells*, 1996] and can be partitioned into three classes broadly defined in terms of expected solubility in simulated cloud-water (acidified freshwater); readily released (<1% total iron), acid-leachable (20–25% total iron) and refractory (~75% total iron)

[*Mackie et al.*, 2006]. Readily released iron appears comparable with the ''instantaneous soluble fraction'' of Fe and Al in natural aerosols [*Buck et al.*, 2006] and perhaps represents ferrihydrite [*Mackie et al.*, 2006]. Previous identifications of ''amorphous iron'' are incorrect and ferrihydrite is a better descriptor of an admittedly poorly characterized iron oxide [*Cornell and Schwertmann*, 2003]. *Cornell and Schwertmann* [2003], and references within, point out that there is no fixed dissolution rate for iron-oxide mineral-specific structures, but that there are consistent trends in the rate of dissolution (using strong acids) that span ~3 orders of magnitude with ferrihydrite $\gg$ hematite > goethite. Mössbauer spectra for soils collected from dust producing regions in Australia, including the area where the October 2002 dust storm originated, show the iron oxides present in the soils to be a mixture of hematite (15–50% of iron present) and goethite (50–85% of iron present) (D. S. Mackie et al., unpublished results, 2007).

[28] In some laboratory-based studies ferrihydrite has been used as a surrogate for the main form of dust-derived iron compound found in atmospheric waters [e.g., *Johansen and Key*, 2006]. However, ferrihydrite is generally found only in young, cool and moist soil environments [*Childs*, 1992]; under warmer, drier conditions it transforms into more stable hematite and goethite via dehydration and structural rearrangement [*Jambor and Dutrizac*, 1998; *Yokoyama and Nakashima*, 2005]. The rate of transformation to either hematite or goethite (the exact product depends largely on temperature and moisture levels) follows first order kinetics and is related to the amount of ferrihydrite left [*Cornell and Schwertmann*, 2003]. The major dust producing regions of the world (the Sahara, Gobi and Australian deserts) are large inland drainage basins within deserts [*Prospero et al.*, 2002] and in Australia, in particular, ancient rocks contribute to highly weathered soils which experience long distance fluvial transport before accumulating as dust source deposits [*McTainsh*, 1989]. Therefore, any ferrihydrite originally present in such source soils is expected to have long since been transformed to hematite or goethite. Ferrihydrite forms from the hydrolysis of Fe(III) solutions [*Childs*, 1992; *Jambor and Dutrizac*, 1998] and any ferrihydrite present in atmospheric aerosols must form secondarily after the dissolution of hematite and goethite such that iron is more likely to be found as hematite, goethite or as ''dissolved'' iron than as ferrihydrite, accounting for the low ''readily released'' or ''instantaneous soluble fraction'' of iron observed in atmospheric aerosols. Thus, models for the dissolution of iron from aeolian dusts based solely on the results from ferrihydrite [e.g., *Johansen and Key*, 2006] will significantly overestimate the actual dissolution of iron from aerosols.

[29] The acid-leachable pool is soluble over a timescale of hours to days in mineral acid solutions of pH <3, while the refractory pool is insoluble under such conditions. The size of the acid-leachable pool of iron is 20–200 times that of the readily released iron, and therefore understanding the extent to which dissolution of this fraction occurs will better inform predictions for iron supply to the ocean. In laboratory-based cloud processing simulations (acidified freshwater, pH 1–5), the dissolution of acid-leachable iron from soils and dusts taken from three arid regions (Australia, the Sahara and the Gobi) occurs in two distinct phases [*Mackie et al.*, 2006; D. S. Mackie et al., unpublished results, 2007]. First there is rapid (hours) release of iron to solution via a reaction with a rate-dependency on the surface area of dust grains (defined by particle size but also surface roughness). Second, a subsequent release of iron to solution occurs more slowly (days) via diffusion and the formation of a leached layer. The release of iron slows as the leached layer increases in thickness and, if the layer remains intact, the release of iron effectively ceases, leaving a refractory portion of iron. However, iron is mainly taken up by phytoplankton from the dissolved form via a ligand-mediated process [*Maldonado et al.*, 2001] and measurements of the inorganic phase of iron can only serve as a guide to the ultimate bioavailability which must be investigated case by case.

2.5. Response of Oceanic Biota to Dust Inputs

[30] Due to the episodic nature of dust supply to the ocean, particularly from Australian sources, it is problematic to directly estimate the response of oceanic biota, although in other oceanic regions, occasionally this biological response has been recorded [*Young et al.*, 1991]. Therefore, satellite remote-sensing has mainly been used to explore the relationship between dust supply and consequent increases in phytoplankton stocks resulting from iron-stimulated algal growth. Two distinct approaches have been applied to the offshore waters of Australasia: *Gabric et al.* [2002] compared satellite time series of Aerosol Optical Depth (AOD) and chlorophyll from SeaWiFS (Sea-viewing Wide Field-of-view Sensor) ocean

color data for subpolar waters south of Australia. In contrast, *Boyd et al.* [2004] identified specific dust storms between 1997 and 2000 (using a land-based network of dust-monitoring stations) and air mass trajectory analysis to identify potential offshore regions where dust was deposited. Dust trajectories were then overlaid on weekly composite satellite-derived chlorophyll fields and examined for elevated chlorophyll (selected images had a 7–14 d lag after each dust storm, the time needed for iron-elevated algal growth rates to result in increased phytoplankton stocks).

[31] Although *Gabric et al.* [2002] reported a strong correlation between AOD and chlorophyll concentrations, *Boyd et al.* [2004] noted no increase in chlorophyll following the dust storms. Significantly, the AOD to chlorophyll relationship reported by *Gabric et al.* [2002] weakened when they introduced a 7–10 d lag; this trend is probably due to the partial removal of autocorrelation between AOD and chlorophyll reported by some remote-sensing studies [*Boyd et al.*, 2004; *Doney et al.*, 2003]. Care in the interpretation of satellite data is also required, as environmental factors other than iron supply, can control phytoplankton growth in early spring, such as underwater light climate [*Boyd et al.*, 2001, 2004].

[32] The period between 1997 and 2000 had relatively low dust activity, whereas in 2002 and 2003 there was a dramatic increase in the DSI_3 (Figure 3). Here we present an analysis of the impact of the 23 October 2002 dust storm on phytoplankton stocks. After the dust plume passed off the Queensland coast, it bifurcated (Figure 5), with dust being deposited into both the HNLC low-iron waters south of New Zealand, and LNLC iron-depleted waters of the Coral Sea (NW of New Zealand) and also into the Gulf of Carpentaria [*Chan et al.*, 2005; *McTainsh et al.*, 2005; *Shao et al.*, 2007]. Dust supply to the former region may stimulate diatoms which are usually iron-limited in these waters [*Boyd et al.*, 2005; *Breviere et al.*, 2006], while in the latter region may have stimulated nitrogen-fixers such as *Trichodesmium* which are iron- and/or iron/P-limited [*Mills et al.*, 2004].

[33] Although *Berman-Frank et al.* [2001] estimated that in 75% of the global ocean, iron availability limits N fixation by *Trichodesmium*, this is now thought to be an overestimate and there is presently considerable debate, from both laboratory [*Hutchins et al.*, 2007], field [*Mills et al.*, 2004] and modeling [*Deutsch et al.*, 2007] studies, as to the factors that limit nitrogen fixers in the LNLC ocean. They provide evidence that different environmental factors may influence the rate of nitrogen fixation including iron/phosphate [*Mills et al.*, 2004], oceanic CO_2 concentrations [*Hutchins et al.*, 2007] and/or N:P stoichiometry in nutrient concentrations [*Deutsch et al.*, 2007]. Hence, the atmospheric supply of dust, with relatively high iron content relative to that for N and P may not necessarily result in a bloom of nitrogen fixers. Soils taken from dust source regions in Australia were found to have ~0.04% N w/w (D. S. Mackie, unpublished data, 2006) and ~3.5% Fe w/w [*Mackie et al.*, 2005]. In the subtropical (ST) waters north of New Zealand (NZ) and east of Australia upper ocean NO_3 concentrations are <2 nM while those of PO_4 are ~50 nM (C. S. Law, manuscript submitted to *Nature*, 2008). Thus, waters where the resident phytoplankton are iron-limited around Australasia are: the HNLC waters south of Australia, and south and east of New Zealand, which in some seasons may be limited by additional factors [*Boyd*, 2002] (e.g., early spring: light, spring Fe + light; late summer: Fe and Si). The same is probably the case for the LNLC waters north of the Tasman Front, which are oligotrophic (Law, submitted manuscript, 2008), but with the caveats above concerning P, N:P, CO_2, etc.

[34] The fallout zone for dust following the October 2002 event has been modeled [*Butler et al.*, 2007; *Shao et al.*, 2007] and is shown in Figure 7 along with TOMS images for 23, 24 and 25 October 2002. Fine details are not visible but the long dust front present in Figure 5 is readily apparent. Deposition did not occur further south than about 40°S (note also the considerable activity of the understudied NW dust pathway, as discussed above). This approximate deposition zone is consistent with the modeled deposition for this event of *Shao et al.* [2007]. Examination of ocean color images from the AQUA satellite for the waters north of New Zealand 7 to 35 d after the October 2002 event revealed no significant increase in chlorophyll concentrations (Figure 8). Here, and throughout, we define a post-deposition bloom as one in which ambient chlorophyll concentrations in either LNLC (0.1 $\mu g\ L^{-1}$) or HNLC (0.3 $\mu g\ L^{-1}$) waters are elevated, for a sustained period (i.e., >7 days), to 1 $\mu g\ L^{-1}$ or greater. Note that the "green" patch between Australia and New Zealand at about 40°S that can be seen in each panel of Figure 8, was present before the dust storm and was not in the fallout path of the dust (Figure 7) and is, therefore, not connected to dust supply. In addition, these waters are north of the STC and so are seldom characterized by limiting dissolved iron concentra-

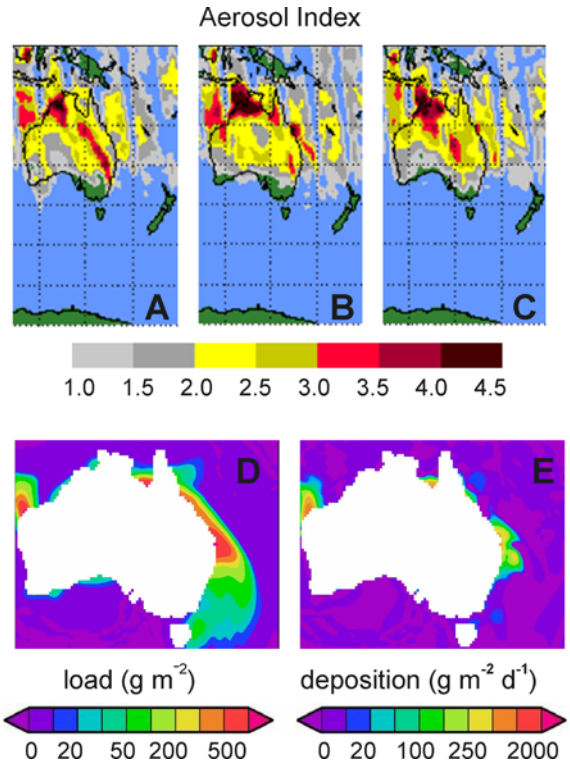

Figure 7. Approximate fallout zone of dust following the 23 October 2002 dust storm event. Figures 7a–7c give TOMS aerosol index for 23, 24, and 25 October 2002, respectively. Figures 7d and 7e (taken from *Shao et al.* [2007]) give modeled dust load and deposition, averaged for the day of 23 October 2002 from 0000–2400 UTC. TOMS images courtesy NASA/GSFC.

tions, and thus blooms are observed there during the spring and summer periods [*Boyd et al.*, 2004].

[35] Moreover, application of an empirically based *Trichodesmium* algorithm, which has been successfully used to detect "ground-truthed" (i.e., from shipboard studies) blooms of these N-fixers [*Westberry et al.*, 2005], revealed no evidence of a bloom east or northeast of Australia (Figure 9). While *Trichodesmium* does not exhibit growth rates like those of diatoms for instance, theoretical maximum growth rates of $\sim$0.9 d^{-1} are now reported [*Rabouille et al.*, 2006] and rates of 0.45 d^{-1} are now considered routine. Given an initial seed population of $\sim$50 *trichomes* L^{-1} (as observed during a survey voyage in these waters in 2006) only 6 divisions would be required (assuming no losses) to achieve the bloom threshold identifiable by the algorithm. This timescale is well within the domain of the images presented in Figure 9.

[36] The alteration of remote-sensing masks, used by *Westberry and Siegel* [2006], for sea surface temperature and water depth (Figure 10) (to increase the areal extent of waters, considered in Figure 9, to include those in which *Trichodesmium* blooms have been observed, such as NW of New Zealand in April 2006 (P. W. Boyd, unpublished observations)) did not alter this conclusion. Note that Figure 10 demonstrates the extent of environmental masking applied to any *Trichodesmium* fields retrieved as a possible caveat to why no obvious *Trichodesmium* blooms were observed in this region. Figure 10 itself contains no information about the actual retrievals, but is made from corresponding maps of SST, bathymetry, and atmospheric correction parameters from SeaWiFS. Minor tweaking of these masks was done to determine if potential bloom signatures were being masked out. The answer was no. That is, no obvious major bloom was produced following the largest dust storm in 40 years.

[37] Two other major dust storm events, in November 2002 and October 2003, were also investigated (data not shown). The former, based on

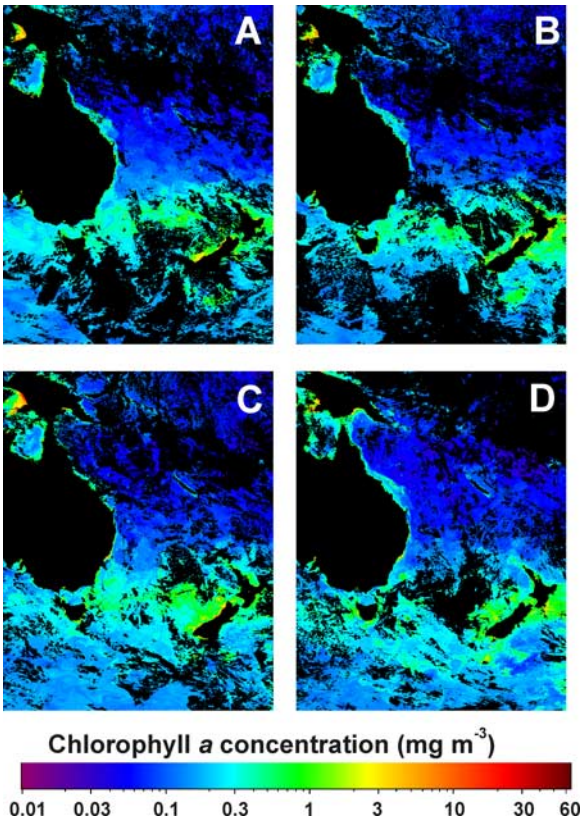

Figure 8. Weekly composite MODIS Aqua images of surface water chlorophyll *a* following the 23 October 2002 dust storm event: (a) 1–8 November, (b) 9–16 November, (c) 17–24 November, and (d) 25 November to 2 December. Images provided by the SeaWiFS Project, NASA/Goddard Space Flight Center, and GeoEye.

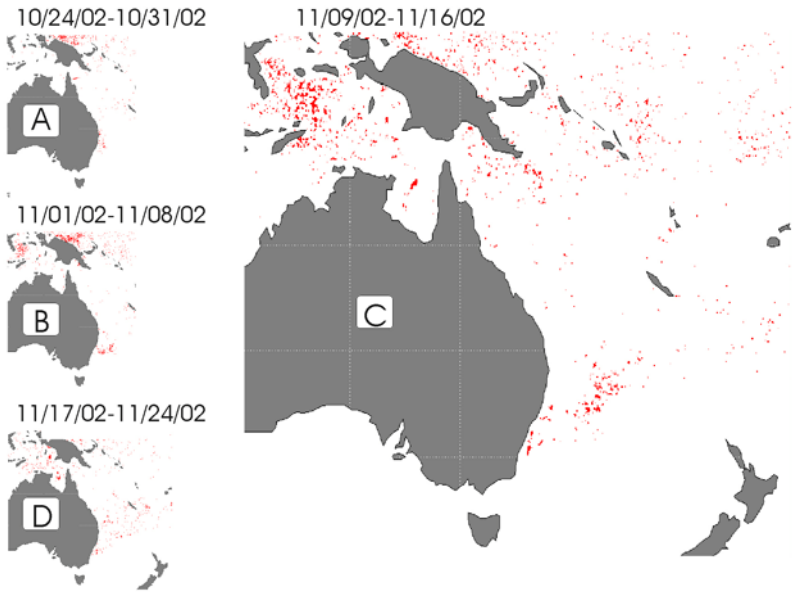

Figure 9. Maps of the occurrence of *Trichodesmium* blooms in the LNLC waters east and northeast of Australia for 4 weeks after the 23 October 2002 dust event. Due to their relatively slow growth rate, a bloom of large areal extent would not be expected before 14–21 days [*Mills et al.*, 2004], and this time period is shown in detail in Figure 9c. The maps are based on the *Trichodesmium* algorithm of *Westberry and Siegel* [2006], but here a modified SST mask is used (all surface waters <21°C are masked as opposed to <23°C, as in the work of *Westberry and Siegel* [2006]). This altered SST mask includes waters northwest of New Zealand in which *Trichodesmium* blooms have been observed recently (P. W. Boyd, unpublished data, 2006). A modified depth mask (waters <50 m deep are masked here, as opposed to those <100 m in the work of *Westberry and Siegel* [2006]) is also applied here as some of the dust plume passed over the relatively shallow Gulf of Carpentaria (see Figure 6). Information on the spatial extent of each type of mask is presented in Figure 10.

Total Ozone Mapping Spectroscopy (TOMS) data, passed south and southeast of Tasmania into HNLC waters. The October 2003 event also may have deposited dust into HNLC waters east of Tasmania and south of New Zealand. Air mass trajectories for each event, overlaid on time-lagged Ocean Color images [after *Boyd et al.*, 2004], revealed no significant increase in chlorophyll concentrations (criteria as above) in these waters 7 to 30 d after the dust storm. These findings are in contrast to those of *Breviere et al.* [2006] who also used TOMS images and air mass trajectories to suggest that dust deposition from a storm in January 2003 may have resulted in increased chlorophyll concentrations (from MODIS) and a consequent drawdown in atmospheric CO_2 in HNLC waters south of Australia.

3. Discussion

3.1. Overview of the Biogeochemistry of Australian Dust

[38] It is evident from this first attempt to order the many processes that contribute to the biogeochemistry of iron in Australian dust that there are many gaps in our knowledge, such that it is difficult to prioritize future research. Perhaps the most striking characteristic of the Australian system is the episodic nature of dust storms, which means that it is important to put each dust event into a temporal context; the response by phytoplankton to a dust storm in early spring will be different from the response in winter or late summer. It is equally important to calculate how much aerosol-derived iron is available to phytoplankton following each storm, and over what timescales (i.e., residence time of the dust in the upper ocean, and dissolution rate over this period). Moreover, local meteorology will control the fate of the dust, i.e., whether it is deposited in subtropical LNLC waters (where N-fixers reside) or subpolar HNLC waters (iron-limited diatoms).

[39] An aqueous medium is essential for any reaction to occur and in the presence of water (e.g., atmospheric moisture and clouds) other key processes, for iron/dust biogeochemistry, that we have identified include particle size, which is an important factor determining iron solubility from mineral dusts [*Baker and Jickells*, 2006; *Bonnet and Guieu*, 2004] and abrasion. Most abrasion of soil occurs

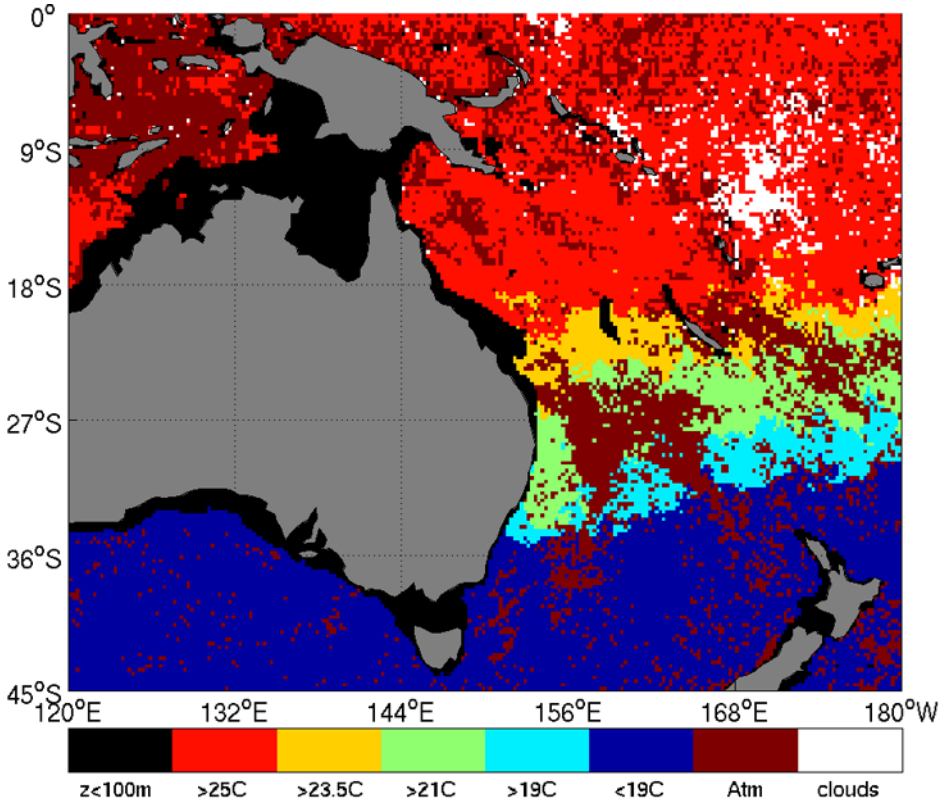

Figure 10. A composite map showing the areal extent of masks applied to the *Trichodesmium* algorithm of *Westberry and Siegel* [2006] for the oligotrophic waters around NE and east Australia during October and November 2002. Three masking schemes are used: for bathymetry (masking any waters shallower than 100 m), SST (masking waters <23°C), and for atmospheric contamination (Atm denotes an additional mask for atmospheric correction of the satellite signal due to high aerosol loading). The SST mask was successively relaxed to waters <19°C. In this case, the large Atm mask was probably due to the eastward passage of the 23 October dust storm offshore. "Clouds" denote areas that were chronically obscured by clouds during the extent of this analysis.

during the initial period of saltation (i.e., during uplift) and produces fine particles [*Bullard et al.*, 2004] that may be more easily transported atmospherically than larger particles. Little is known about abrasion during the transport of entrained dust (referred to as attrition) but early indications are that such abrasion processes can also redistribute more soluble forms of iron onto smaller grains [*Mackie et al.*, 2006]. Interactions with cloud-water [*Baker et al.*, 2003; *Mackie et al.*, 2005; *Meskhidze et al.*, 2005; *Spokes et al.*, 1994] and photochemistry [*Hand et al.*, 2004; *Siefert et al.*, 1999; *Zhuang et al.*, 1992b] can also influence the dissolution of iron from Australian dust and therefore affect the supply of bioavailable iron to phytoplankton.

[40] Another significant outcome of this synthesis is that the enhancement of iron-solubility by each of the above mechanisms is difficult to measure in isolation. Hence dissolution experiments in mineral acid solutions over long periods (days) have been used to set an upper bound on how much iron is potentially bio-available [*Mackie et al.*, 2005; *Spokes et al.*, 1994]. These experiments have also elucidated a mechanism for the dissolution of iron from dust that occurs in two stages over timescales of hours and weeks, respectively (D. S. Mackie et al., unpublished manuscript, 2008). *Boyd et al.* [2005] propose two distinct mechanisms for dust dissolution in the surface ocean: physico-chemically mediated (hours) and microbial/photo-chemically mediated (weeks) during the residence of aerosol particles in the upper ocean. This is consistent with the findings from a mesoscale iron biogeochemical study (FeCycle) in unperturbed HNLC Australasian waters where "an average residence time of particles in the mixed layer of ~100 days" is calculated [*Frew et al.*, 2006]. A "fractional mean residence time" of (6–62 days) for total (dissolved and particulate) iron is also reported for waters directly under the path of Saharan dust plumes [*Croot et al.*, 2004] and the residence time for dust

in surface waters of the Sargasso Sea is calculated to be ~18 days [*Jickells*, 1999].

[41] As noted above, these mechanisms with moderate to slow dissolution rates contrast with the immediate availability of acidified iron(II) in mesoscale perturbation experiments (e.g., SOIREE, IRONEX and FeCycle) and may account for observed differences in phytoplankton responses to the natural (i.e., dust events) and purposeful addition of iron in such experiments [see *Boyd et al.*, 2007].

3.2. Dust Emission and Deposition: A Comparison of Southern Hemisphere Sources

[42] It is evident that the relatively detailed measurements on dust biogeochemistry for Australia are the most comprehensive in the Southern Hemisphere. It is therefore valuable to assess whether they are broadly representative of other important dust-producing regions south of the Equator, which have had less research effort directed at them. In the following sections we compare how the main characteristics of the biogeochemistry of Australian dust relates to Patagonian and southern African dusts. We then compare and contrast dust processes between the Northern and Southern Hemispheres.

[43] The relative importance of Southern Hemisphere sources of dust, with respect to iron supply to polar phytoplankton, is sometimes assessed on the basis of how much dust is transported to Antarctica [*Wolff et al.*, 2006]. The major dust source regions in the Southern Hemisphere are Australia [*McTainsh et al.*, 2005], Patagonia [*Gaiero et al.*, 2004] and southern Africa [*Piketh et al.*, 2000]. Minor sources include the Bolivian Altiplano (14–21°S), Buenos Aires Province and W Argentina (~35°S) [*Gaiero et al.*, 2004]. Antarctica is probably only a minor source because prevailing katabatic winds long ago removed any large deposits of dust and pedological processes in the limited ice-free areas to produce fresh soil are very slow [*Campbell and Claridge*, 1987]. The relative contribution of each source to dust in Antarctic ice cores remains a subject of debate [*Basile et al.*, 1997; *Revel-Rolland et al.*, 2006; *Tanaka and Chiba*, 2006]. However, the strong westerly winds that limit the transport of dust to Antarctica [*Trenberth et al.*, 1990], should not be equated to a lack of dust supply to the Ocean.

[44] An additional consideration concerning the bioavailability of iron is presence of combustion products in the atmosphere interacting with dust and iron. For example, iron in Saharan dust over the Sargasso Sea has greater solubility if it has mixed with air masses from North America carrying high levels of fossil fuel combustion products [*Sedwick et al.*, 2007]. In particular for the Australian case, the impact of smoke from the frequent natural bushfires (plumes of which are clearly seen passing through the dust plume in Figures 5a and 5b) has been previously unstudied, so we currently have a program underway to investigate this issue.

[45] The main focus of dust studies in Patagonia has been its potential important role in iron-enrichment of Southern Ocean waters during the LGM [*Wolff et al.*, 2006] and research has mainly been on dust transport processes to sites in Antarctica (e.g., Dome C, Vostok) where deep ice cores have been taken. In southern Africa, most of the research has addressed the effect of dust and aerosols (especially those produced by biomass burning) on the climate (rainfall and temperature) over the land itself [*Piketh et al.*, 2002; *Tyson et al.*, 1996].

[46] As discussed above, two key factors that control dust-derived iron delivery to the surface ocean are (1) the size of a dust event and (2) the frequency and duration of a dust event. Events that transport dust from southern Africa occur regularly, every 11 d or so, with each event lasting ~3 d [*Piketh et al.*, 2000]. The annual dust flux eastward from southern Africa to surface waters of the southern Indian Ocean is about 45 Tg a^{-1} with a further 25 Tg a^{-1} westward into the southern Atlantic [*Tyson and D'Abreton*, 1998; *Tyson et al.*, 1996]. Atmospheric deposition of soils from Patagonia to the Patagonian Argentine continental shelf (0.8×10^6 km^2) is estimated at 30 Tg a^{-1} [*Gaiero et al.*, 2003]. Emission of dust from Patagonia occurs regularly throughout the year, although there is significant seasonal variation in dust deposition rates onto the Atlantic coastline from 0.3 to 8.1 g m^{-2} $month^{-1}$ [*Gaiero et al.*, 2003]. Australian dust supply to the South Pacific is less, 4–7 Tg a^{-1} [*Knight et al.*, 1995], and as discussed above, is episodic. Thus, each Southern Hemisphere dust source region has distinctive characteristics that mean that no particular one is representative of the region as a whole.

[47] Southern African dust that enters the ocean is largely (>90%) deposited in the southern Indian Ocean along ~35°E with only 4% entering the South Atlantic [*Garstang et al.*, 1996]. Around 22% of air masses originating over southern Africa are transported over the Tasman Sea to the south of New Zealand in winter (transport is insignificant

during summer) [*Sturman et al.*, 1997] but <6% of back trajectories from the Dome C site in Antarctica (75°S 123°E) originating in southern Africa [*Lunt and Valdes*, 2001]. About a third of southern Africa dust exports are deposited in iron-rich coastal waters (i.e., with little impact on the biota), with ~50% reaching the 70°E meridian (~3500 km from the coast) [*Piketh et al.*, 2000]. Patagonian dust has been identified in Antarctic ice cores at Dome C (75°S 123°E) [*Basile et al.*, 1997; *Wolff et al.*, 2006] and nearby Vostok (78°S 106°E) [*Delmonte et al.*, 2004b]. Back trajectory analysis shows >30% of trajectories to Dome C originate in Patagonia, and follow the circumpolar zonal winds [*Lunt and Valdes*, 2001]. However, from the same back trajectories, it appears that Patagonian dust is seldom deposited to the north of 40°S.

[48] While ice core studies of dust deposition in Antarctica have made major contributions to our knowledge of long distance dust transport during the geological past, many of the studies attempting to provenance the dust share the methodological weakness of using only a small number of samples to identify potential source areas. For example *Grousset et al.* [1992] isotopically fingerprinted (143/144 Nd to 87/86 Sr ratios) soil from the entire Australian continent using samples from just two locales. One of these, in the Great Sandy Desert, falls along the NW dust path (Figure 6) and would not be expected to contribute dust to Antarctica. While *Basile et al.* [1997] used a single sample of loess to characterize (also by Nd/Sr ratios) New Zealand soils. Given that New Zealand straddles two tectonic plates and is highly volcanic, it may be that there is considerable variation in soil isotopic composition that would not be detected by examination of such a limited sample set.

3.3. Impact of Deposited Dust on Biota in the Southern Hemisphere

[49] Dust originating from southern Africa typically supplies 0.99 mg Fe m^{-2} d^{-1} per dust event [*Piketh et al.*, 2000] into the waters of the South Indian Ocean between 30°S 50°E and 50°S 70°E (an area of $\sim 4 \times 10^6$ km^2). The South Indian Ocean is characterized by discrete regions (total areal extent $\sim 1.5 \times 10^6$ km^2) of enhanced CO_2 uptake [*Takahashi et al.*, 1997] and some of these have been linked to oceanic deposition of dust plumes from southern Africa [*Piketh et al.*, 2000]. However, the areas of increased CO_2 uptake are close to the Crozet (46°S 51°E) and Kerguelen (49°S 70°E) island plateaus, and in both cases the Antarctic Circumpolar Current (ACC) results in upwelling [*Read et al.*, 1995] which enriches surface waters with iron [*Blain et al.*, 2007; *Holm-Hansen et al.*, 2005]. The extent of the influence of southern African dust on biota is therefore unclear. Patagonian dust is estimated to supply 1–4 mg "leachable" (in 0.5N HCl) Fe m^{-2} a^{-1} to HNLC waters of the subpolar South Atlantic Ocean [*Gaiero et al.*, 2003]. However, upwelling of the ACC in the Scotia Sea enriches surface iron and nutrients [*Holm-Hansen et al.*, 2005] making it difficult to assess the direct impact of Patagonian dust on biota. On the other hand, *Meskhidze et al.* [2007, paragraph 1] conclude that "upwelling of nutrient-rich waters due to mesoscale frontal dynamics is the major source of bioavailable Fe controlling biological activity in this region." As additional data is collected conclusions such as this about the balance of "iron from above" versus "iron from below" may change. In contrast, the Australian-South Pacific sector of the Southern Ocean has negligible upwelling and is remote from land. It may therefore be a less complex system better suited for the study of how dust processes influence ocean biota.

3.4. Southern Hemisphere Data Coverage: Dust Deposition

[50] Dust processes in the Southern Hemisphere are understudied relative to those in the Northern Hemisphere. The SEAREX program of 1979–1987 [*Prospero et al.*, 1989] is the only major study to include numerous sampling sites south of the Equator. Remote-sensing is now providing valuable information on dust sources. For example, maps for dust storm activity produced from TOMS, MODIS and SeaWiFS data have good agreement with ground-based observations [*Darmenova et al.*, 2005; *Washington et al.*, 2003]. Even though TOMS offers the longest satellite record of dust activity over the Australian continent (1979 to date), the TOMS record is incomplete, and may miss many of the common haboob-type events (where there is a rapidly moving cold front and dust is entrained at <500 m), leading to the erroneous conclusion that dust output from Australia is negligible [*McGowan et al.*, 2005].

3.5. Modeling of Dust Deposition for the Australian Region

[51] *Wagener et al.* [2008] report extremely low measured dust fluxes to the SE Pacific east of

Table 2. Locations of Data Sources Used to Constrain and Validate ModelE for Global Dust Emissions for Each Ocean Basin[a]

Data Set	Type	Total	NP	NA	NI	Total North	SP	SA	SI	SO	Total South
AERONET[b]	O	17	4	6	3	13	4	0	0	0	4
AVHRR[c]	O	3	0	2	1	3	0	0	0	0	0
TOMS[d]	O	4	0	3	1	4	0	0	0	0	0
Miami[e]	F	19	6	7	0	13	6	0	0	0	6
Ginoux[f]	F	3[e] (12)	1[g] (5)	2[g] (2)	0 (0)	3 (7)	0 (5)	0 (0)	0 (0)	0 (0)	0 (5)
DIRTMAP[h]	S	47	12	21	6	39	3	4	0	1	8
Total		93	23	41	11	75	13	4	0	1	18

[a] ModelE: *Cakmur et al.* [2006]. NP, North Pacific; NA, North Atlantic; NI, North Indian; SP, South Pacific; SA, South Atlantic; SI, South Indian). Type of measurement technique: O, optical and remote sensing; F, dust collected at ground on filters; S, sediment trap. (Note that most of the Ginoux data appear to be re-reporting of the Prospero data.)
[b] AErosol RObotic NETwork.
[c] Advanced Very High Resolution Radiometer.
[d] Total Ozone Mapping Spectrometer.
[e] *Prospero et al.* [1987, 1989].
[f] *Ginoux et al.* [2001]. Unique sites only. ModelE uses data for only 12 of the 16 sites reported in the source but of these; 9 are themselves re-reporting of the data from Prospero (footnote e) and are given in parentheses. The source gives data for two new land-based sites in southern Europe and one new ocean site in the Aleutians.
[g] Land-based sites.
[h] *Tegen et al.* [2002]. Compilation of 48 sites from the total of 73 in the DIRTMAP database.

Tahiti and to the Southern Ocean south of Kerguelen Island (6 and 22 ng m^{-2} d^{-1}, respectively) and comment that these values are ~100 times lower than previous predictions from global modeling simulations. These models are largely based on the more abundant Northern Hemisphere data, yet they have been widely used to predict both dust and bioavailable iron deposition into the Southern Ocean [*Cassar et al.*, 2007]. This approach has inherent dangers: "...From there, it is but a short step to the astonishing evocation of a relationship between seasonality of chlorophyll biomass and of modeled dust deposition in the Southern Ocean" [*Longhurst*, 2006, p. 72].

[52] In contrast, the DSI related meteorological data available for Australia make the validation of regional dust deposition models viable. This has recently been done by *Shao et al.* [2007], who modeled the dust load of the 23 October 2002 storm using a regional dust model. They found that modeled and measured dust loads were similar: 5 and 4.85 Tg, respectively. In contrast, most global dust models have particular difficulty in predicting accurately Australian dust emissions and the extent/location of dust source areas because of the spatial complexity of dust source areas and the episodicity of Australian dust processes. Some models overestimate the dust source strength of the Australian continent [e.g., *Bauer et al.*, 2004], and their outputs do not compare well with satellite records of dust transport [*Perlwitz et al.*, 2001]. Zender's DEAD model [*Zender et al.*, 2003] works relatively well at identifying the major dust source regions in Australia because it describes better soil erodibility constraints upon dust emissions than most models.

[53] Some models for global dust processes are almost exclusively based on Northern Hemisphere data. For example, the dust component of the NASA-Goddard Atmospheric General Circulation Model, ModelE [*Cakmur et al.*, 2006; *Miller et al.*, 2006], is constrained by measurements of whole region remotely sensed aerosol optical depth and also by particulate loads collected by high-volume filters and sediment traps from 93 oceanic and 3 land sites, yet only 18 of the sites are in the Southern Hemisphere; 13 are in the South Pacific (Table 2). The SEAREX data set [*Prospero et al.*, 1989] has been used to validate most global dust deposition models to date. However, both the absolute DSI for Australia and the year to year variation in the DSI during the SEAREX program was low compared to the decades both before and after (see Figure 3). There is not yet sufficient data to determine the "normal" DSI for Australia and the scarcity of ground-based observations of dust activity in the Southern Hemisphere makes it difficult to asses the reliability of the global dust emission model simulations for this region.

[54] A potentially promising approach to modeling the impact of dust deposition on phytoplankton in offshore waters is to use detailed region-specific data to both place constraints on conditions for bloom formation, and to identify gaps in our knowledge. For example, using data from our

Table 3. Comparison of Properties Influencing the Delivery of Dust-Derived Iron to the Oceans of the Northern and Southern Hemispheres

Property	Northern	Southern
Land 30–70° ($\times 10^6$ km^2)	63	8
Ocean 30–70° ($\times 10^6$ km^2)	50	104
Proportion of total oceanic dust deposition	>80%	<20%
Timing of dust intrusions over the ocean	Sahara: Regular year-round emission, spring/summer peak [*Prospero et al.*, 2002]. Gobi: Regular year-round emission, spring/summer peak [*Xuan*, 2005].	Australia: Irregular, spring/summer only [*Ekström et al.*, 2004]. Southern Africa: Regular year-round emission, every ~11 days [*Piketh et al.*, 2000]. Patagonia: Year-round emission, spring/summer peak [*Gaiero et al.*, 2003].
Transport time	Sahara to Barbados 5–7 days [*Colarco et al.*, 2003b] Gobi to US mainland ~7 days [*VanCuren and Cahill*, 2002].	(to Antarctica) Australia 6.5 days Patagonia 5.5 days Southern Africa 8.5 days [*Krinner and Genthon*, 2003].
Solubility enhancing pollutants (SOx NOx)	High [*Meskhidze et al.*, 2003; *Sasakawa and Uematsu*, 2005]	Low [*Ayers et al.*, 1997].
Photochemistry (mean monthly insolation Wm^{-2})	405 ± 40 at 15°N	360 ± 150 at 30°S 187 (0–530) at 70°S
Relative areal extent of LNLC iron limited waters.	1	1.5 (*Trichodesmium*) [*Westberry and Siegel*, 2006]
Relative areal extent of HNLC iron limited waters.	1	4 (diatom species) [*Boyd et al.*, 2007]

synthesis as inputs to a simple box model (D. S. Mackie et al., unpublished results, 2007) we explore the effects of a dust storm similar in size to the 23 October 2002 event on ocean productivity. Such a storm results in predicted values for dissolved iron in HNLC surface waters up to 3000 km offshore from Australia that range from 0.04 (lower bound) to 0.60 nM (upper bound); concentrations of 0.3 nM Fe and above will significantly stimulate phytoplankton growth [*Boyd et al.*, 2001] above ambient. Parameters such as the half-decrease distance for dust transportation, the time-scale for iron dissolution from dust in surface waters, and the half-life of dissolved iron in the ocean are too poorly known in the Australasian region to progress beyond stating an upper and lower bound for oceanic iron supply.

3.6. Comparison of Northern and Southern Hemisphere Dust Processes

[55] Interhemispheric differences in factors likely to influence the dissolution of iron from dust are presented in Table 3. Global patterns of predominant winds divide each hemisphere into three latitudinal zones: Trade winds (0°–30°), Westerlies (30°–60°) and Polar Easterlies (60°–90°). If it is assumed, as a first approximation, that there is little transport between these zones, then dust sources on the land area between 30°S and 60°S (5×10^6 km^2) supply most of the eolian dust deposited to the oceans in this zone (89×10^6 km^2). In the Northern Hemisphere the land and ocean areas between 30°N–60°N are 48×10^6 km^2 and 46×10^6 km^2, respectively. Dust is emitted from the Gobi and Sahara almost year-round while emissions from Australia and, to a lesser extent, Patagonia, have a pronounced seasonality. These differences alone have undoubtedly contributed to the establishment of the large HNLC areas in the Southern Ocean and further accentuate the importance of dust processes in the Southern Hemisphere. Also, Northern Hemisphere dust sources are at lower latitudes than those in the Southern Hemisphere (~15°N versus ~30°S) and entrained dust experiences greater insolation during transport, with greater potential for dissolution of iron via photoreduction reactions initiated by high energy irradiance [*Borer et al.*, 2005; *Tagliabue and Arrigo*, 2006]. The impact that each of these processes has on the bioavailability of iron varies, and the level of current understanding of each process is summarized in Figure 11.

[56] Large dust storms alone do not initiate blooms, but do increase the overall ocean iron inventory. Other factors also contribute to the control of bloom initiation in LNLC waters (i.e., Fe/P/CO_2/N and P stoichiometry). In HNLC waters

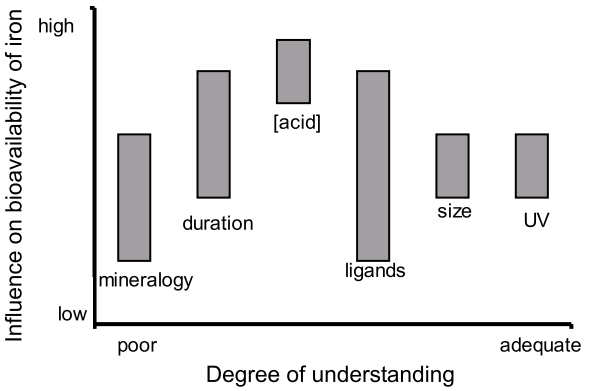

Figure 11. A semiquantitative assessment of our current level of understanding of atmospheric processes (introduced in Figure 1) in relation to their relative influence on the bioavailability of iron in surface ocean waters. For example, mineralogy probably has a low to moderate impact on the bioavailability of iron, as the particular forms of iron present in aeolian dust show little variation though, as noted, models do not always take account of this. Nevertheless, our current understanding of the influence of mineralogy is poor. Time denotes the timescale of atmospheric processing during dust transport and may include multiple cycles of processing. The label [acid] refers to the acidity of the medium in which the dust is transported (such as clouds): this has a major effect on bioavailability, but the environmental conditions inside clouds are not well understood. Ligands denotes the solubility-enhancing properties of iron-binding ligands and indicates that little is known about ligand interactions (rainwater) with dust in the atmosphere. Size refers to the influence of particle size, an important contributor toward bioavailability that is becoming better understood. UV refers to the well-defined impact of UV irradiation. Note that bioavailability may have no direct relationship to the biological response.

limiting factors may be Fe, light and even Si [*Boyd*, 2002]. Further, the seasonal cycle in each of these limiting factors makes the specific timing of the atmospheric Fe deposition event become important. Better information is required on the relative role of the atmosphere and ocean on influencing iron biogeochemistry and how their relative influences might change in the future due to climate change.

[57] A further fundamental issue is that some models for the dissolution of iron from dust, based on Northern Hemisphere data, explicitly include the solubility enhancing effect of pollutants like SO_X and NO_X [*Fan et al.*, 2006; *Mahowald et al.*, 2005; *Meskhidze et al.*, 2005]. However, levels of such anthropogenic pollutants are relatively low in the modern atmosphere of the Southern Hemisphere [*Ayers et al.*, 1997] and were low globally during the LGM. Therefore, future modeling efforts on dust deposition into the Southern Ocean in the geological past require both parameterization that reflects the pristine environment at that time, and better data sets for each of the Southern Hemisphere dust source regions.

Appendix A: DSI_3

[58] The Dust Storm Index (DSI_3) is calculated using equation (A1):

$$DSI_3 = \sum_{i=1}^{n} [(5 \times SD) + MD + (0.05 \times LDE)] \qquad (A1)$$

DSI_3 is Dust Storm Index at n stations where i is the ith value of n stations for i = 1 to n. The number of stations (n) is the total number of stations recording a dust event observation in each time period. 109 stations have continuous records and a further ~100 stations have partial or sporadic records.

[59] SD is severe dust storm: visibility <200 m (daily maximum weather codes: 33, 34, 35). MD is moderate dust storm: visibility 200–1000 m (daily maximum weather codes: 30, 31, 32 and 98). LDE is local dust event: some dust activity but no negligible change to visibility (daily maximum weather codes: 07 and 08).

[60] Weather codes are as defined by the *World Meteorological Organization* [1998] and weather code 09 events have been reassigned as 07s or 30 to 35s, dependent on visibility criteria.

Acknowledgments

[61] D. M. was funded by the Royal Society of New Zealand Marsden Fund, project UOO215. GMcT and NT were supported by an Australian Research Council Discovery Grant. P.W.B. acknowledges support from both the Marsden Fund and the PGSF Coasts and Oceans OBI. Thanks to Kenn Tews for assistance with DSI data analysis. We gratefully acknowledge the NOAA Air Resources Laboratory (ARL) for the HYSPLIT transport and dispersion model (http://www.arl.noaa.gov/ready.html).

References

Ayers, G. P., J. M. Cainey, R. W. Gillett, and J. P. Ivey (1997), Atmospheric sulphur and cloud condensation nuclei in marine air in the Southern Hemisphere, *Philos. Trans. R. Soc. London, Ser. B*, *352*(1350), 203–211, doi:10.1098/rstb.1997.0015.

Baker, A. R., and T. D. Jickells (2006), Mineral particle size as a control on aerosol iron solubility, *Geophys. Res. Lett.*, *33*, L17608, doi:10.1029/2006GL026557.

Baker, A. R., S. D. Kelly, K. F. Biswas, M. Witt, and T. D. Jickells (2003), Atmospheric deposition of nutrients to the Atlantic Ocean, *Geophys. Res. Lett.*, *30*(24), 2296, doi:10.1029/2003GL018518.

Baker, A. R., T. D. Jickells, M. Witt, and K. L. Linge (2006), Trends in the solubility of iron, aluminium, manganese and phosphorus in aerosol collected over the Atlantic Ocean, *Mar. Chem.*, *98*(1), 43–58, doi:10.1016/j.marchem.2005.06.004.

Basile, I., F. E. Grousset, M. Revel, J. R. Petit, P. E. Biscaye, and N. I. Barkov (1997), Patagonian origin of glacial dust deposited in East Antarctica (Vostok and Dome C) during glacial stages 2, 4 and 6, *Earth Planet. Sci. Lett.*, *146*(3–4), 573–589, doi:10.1016/S0012-821X(96)00255-5.

Bates, T. S., B. J. Huebert, J. L. Gras, F. B. Griffiths, and P. A. Durkee (1998), International Global Atmospheric Chemistry (IGAC) Project's First Aerosol Characterization Experiment (ACE 1): Overview, *J. Geophys. Res.*, *103*(D13), 16,297–16,318.

Bauer, S. E., Y. Balkanski, M. Schulz, D. A. Hauglustaine, and F. Dentener (2004), Global modeling of heterogeneous chemistry on mineral aerosol surfaces: Influence on tropospheric ozone chemistry and comparison to observations, *J. Geophys. Res.*, *109*, D02304, doi:10.1029/2003JD003868.

Berman-Frank, I., J. T. Cullen, Y. Shaked, R. M. Sherrell, and P. G. Falkowski (2001), Iron availability, cellular iron quotas, and nitrogen fixation in *Trichodesmium*, *Limnol. Oceanogr.*, *46*(6), 1249–1260.

Berthier, S., P. Chazette, P. Couvert, J. Pelon, F. Dulac, F. Thieuleux, C. Moulin, and T. Pain (2006), Desert dust aerosol columnar properties over ocean and continental Africa from Lidar in-Space Technology Experiment (LITE) and Meteosat synergy, *J. Geophys. Res.*, *111*, D21202, doi:10.1029/2005JD006999.

Blain, S., et al. (2007), Effect of natural iron fertilization on carbon sequestration in the Southern Ocean, *Nature*, *446*(7139), 1070–1074, doi:10.1038/nature05700.

Boers, R., G. P. Ayers, and J. L. Gras (1994), Coherence between seasonal variation in satellite-derived cloud optical depth and boundary-layer CCN concentrations at a midlatitude Southern Hemisphere station, *Tellus, Ser. B*, *46*(2), 123–131, doi:10.1034/j.1600-0889.1994.t01-1-00004.x.

Bonnet, S., and C. Guieu (2004), Dissolution of atmospheric iron in seawater, *Geophys. Res. Lett.*, *31*, L03303, doi:10.1029/2003GL018423.

Borer, P. M., B. Sulzberger, P. Reichard, and S. M. Kraemer (2005), Effect of siderophores on the light-induced dissolution of colloidal iron(III) (hydr)oxides, *Mar. Chem.*, *93*(2–4), 179–193, doi:10.1016/j.marchem.2004.08.006.

Bowler, J. M. (1976), Aridity in Australia—Age, origins and expression in aeolian landforms and sediments, *Earth Sci. Rev.*, *12*(2–3), 279–310, doi:10.1016/0012-8252(76)90008-8.

Boyd, P. W. (2002), Environmental factors controlling phytoplankton processes in the Southern Ocean, *J. Phycol.*, *38*(5), 844–861.

Boyd, P. W., A. C. Crossley, G. R. DiTullio, F. B. Griffiths, D. A. Hutchins, B. Queguiner, P. N. Sedwick, and T. W. Trull (2001), Control of phytoplankton growth by iron supply and irradiance in the subantarctic Southern Ocean: Experimental results from the SAZ project, *J. Geophys. Res.*, *106*(C12), 31,573–31,584.

Boyd, P. W., G. McTainsh, V. Sherlock, K. Richardson, S. Nichol, M. Ellwood, and R. Frew (2004), Episodic enhancement of phytoplankton stocks in New Zealand subantarctic waters: Contribution of atmospheric and oceanic iron supply, *Global Biogeochem. Cycles*, *18*, GB1029, doi:10.1029/2002GB002020.

Boyd, P. W., et al. (2005), FeCycle: Attempting an iron biogeochemical budget from a mesoscale SF_6 tracer experiment in unperturbed low iron waters, *Global Biogeochem. Cycles*, *19*, GB4S20, doi:10.1029/2005GB002494.

Boyd, P. W., et al. (2007), Mesoscale iron enrichment experiments 1993–2005: Synthesis and future directions, *Science*, *315*(5812), 612–617, doi:10.1126/science.1131669.

Breviere, E., N. Metzl, A. Poisson, and B. Tilbrook (2006), Changes of the oceanic CO_2 sink in the eastern Indian sector of the Southern Ocean, *Tellus, Ser. B*, *58*(5), 438–446, doi:10.1111/j.1600-0889.2006.00220.x.

Buck, C. S., W. M. Landing, J. A. Resing, and G. T. Lebon (2006), Aerosol iron and aluminum solubility in the northwest Pacific Ocean: Results from the 2002 IOC cruise, *Geochem. Geophys. Geosyst.*, *7*, Q04M07, doi:10.1029/2005GC000977.

Bullard, J. E., and G. McTainsh (2003), Aeolian-fluvial interactions in dryland environments: Examples, concepts and Australia case study, *Prog. Phys. Geogr.*, *27*(4), 471–501, doi:10.1191/0309133303pp386ra.

Bullard, J. E., G. H. McTainsh, and C. Pudmenzky (2004), Aeolian abrasion and modes of fine particle production from natural red dune sands: An experimental study, *Sedimentology*, *51*(5), 1103–1125, doi:10.1111/j.1365-3091.2004.00662.x.

Bullard, J. E., G. H. McTainsh, and C. Pudmenzky (2007), Factors affecting the nature and rate of dust production from natural dune sands, *Sedimentology*, *54*(1), 169–182, doi:10.1111/j.1365-3091.2006.00827.x.

Butler, H. J., W. L. Hogarth, and G. H. McTainsh (2001), Effects of spatial variations in source areas upon dust concentration profiles during three wind erosion events in Australia, *Earth Surf. Processes Landforms*, *26*(10), 1039–1048, doi:10.1002/esp.235.

Butler, H. J., Y. P. Shao, J. Leys, and G. H. McTainsh (2007), Modelling wind erosion at national and regional scales, National Monitoring and Evaluation Framework, 38 pp., Natl. Land and Water Resour. Audit, Canberra.

Cakmur, R. V., R. L. Miller, J. Perlwitz, I. V. Geogdzhayev, P. Ginoux, D. Koch, K. E. Kohfeld, I. Tegen, and C. S. Zender (2006), Constraining the magnitude of the global dust cycle by minimizing the difference between a model and observations, *J. Geophys. Res.*, *111*, D06207, doi:10.1029/2005JD005791.

Calvo, E., C. Pelejero, G. A. Logan, and P. De Deckker (2004), Dust-induced changes in phytoplankton composition in the Tasman Sea during the last four glacial cycles, *Paleoceanography*, *19*, PA2020, doi:10.1029/2003PA000992.

Campbell, I. B., and G. C. C. Claridge (1987), *Antarctica: Soils, Weathering Processes and Environment*, Elsevier, Amsterdam.

Cassar, N., M. L. Bender, B. A. Barnett, S. Fan, W. J. Moxim, H. Levy, II, and B. Tilbrook (2007), The Southern Ocean biological response to aeolian iron deposition, *Science*, *317*(5841), 1067–1070, doi:10.1126/science.1144602.

Chan, Y. C., G. McTainsh, J. Leys, H. McGowan, and K. Tews (2005), Influence of the 23 October 2002 dust storm on the air quality of four Australian cities, *Water Air Soil Pollut.*, *164*(1–4), 329, doi:10.1007/s11270-005-4009-0.

Charlson, R. J., J. E. Lovelock, M. O. Andreae, and S. G. Warren (1987), Oceanic phytoplankton, atmospheric sulfur, cloud albedo and climate, *Nature*, *326*(6114), 655–661, doi:10.1038/326655a0.

Chepil, W. S., and N. P. Woodruff (1957), Sedimentary characteristics of dust storms; Part II, Visibility and dust concentration, *Am. J. Sci.*, *255*(2), 104–114.

Childs, C. W. (1992), Ferrihydrite—A review of structure, properties and occurrence in relation to soils, *Z. Pflanzen. Bodenk.*, *155*(5–6), 441–448, doi:10.1002/jpln.19921550515.

Chuang, P. Y., R. M. Duvall, M. M. Shafer, and J. J. Schauer (2005), The origin of water soluble particulate iron in the Asian atmospheric outflow, *Geophys. Res. Lett.*, *32*, L07813, doi:10.1029/2004GL021946.

Colarco, P. R., et al. (2003a), Saharan dust transport to the Caribbean during PRIDE: 2. Transport, vertical profiles, and deposition in simulations of in situ and remote sensing observations, *J. Geophys. Res.*, *108*(D19), 8590, doi:10.1029/2002JD002659.

Colarco, P. R., O. B. Toon, and B. N. Holben (2003b), Saharan dust transport to the Caribbean during PRIDE: 1. Influence of dust sources and removal mechanisms on the timing and magnitude of downwind aerosol optical depth events from simulations of in situ and remote sensing observations, *J. Geophys. Res.*, *108*(D19), 8589, doi:10.1029/2002JD002658.

Cornell, R. M., and U. Schwertmann (2003), *The Iron Oxides: Structure, Properties, Reactions, Occurrences and Uses*, 2nd ed., 664 pp., Wiley-VCH, Weinheim, Germany.

Croot, P. L., P. Streu, and A. R. Baker (2004), Short residence time for iron in surface seawater impacted by atmospheric dry deposition from Saharan dust events, *Geophys. Res. Lett.*, *31*, L23S08, doi:10.1029/2004GL020153.

Cropp, R. A., A. J. Gabric, G. H. McTainsh, R. D. Braddock, and N. Tindale (2005), Coupling between ocean biota and atmospheric aerosols: Dust, dimethylsulphide, or artifact?, *Global Biogeochem. Cycles*, *19*, GB4002, doi:10.1029/2004GB002436.

Darmenova, K., I. N. Sokolik, and A. Darmenov (2005), Characterization of east Asian dust outbreaks in the spring of 2001 using ground-based and satellite data, *J. Geophys. Res.*, *110*, D02204, doi:10.1029/2004JD004842.

Delmonte, B., J. R. Petit, K. K. Andersen, I. Basile-Doelseh, V. Maggi, and V. Y. Lipenkov (2004a), Dust size evidence for opposite regional atmospheric circulation changes over east Antarctica during the last climatic transition, *Clim. Dyn.*, *23*(3–4), 427–438, doi:10.1007/s00382-004-0450-9.

Delmonte, B., I. Basile-Doelsch, J. R. Petit, V. Maggi, M. Revel-Rolland, A. Michard, E. Jagoutz, and F. Grousset (2004b), Comparing the Epica and Vostok dust records during the last 220,000 years: Stratigraphical correlation and provenance in glacial periods, *Earth Sci. Rev.*, *66*(1–2), 63–87, doi:10.1016/j.earscirev.2003.10.004.

Desboeufs, K. V., A. Sofikitis, R. Losno, J. L. Colin, and P. Ausset (2005), Dissolution and solubility of trace metals from natural and anthropogenic aerosol particulate matter, *Chemosphere*, *58*(2), 195–203, doi:10.1016/j.chemosphere.2004.02.025.

Deutsch, C., J. L. Sarmiento, D. M. Sigman, N. Gruber, and J. P. Dunne (2007), Spatial coupling of nitrogen inputs and losses in the ocean, *Nature*, *445*(7124), 163–167, doi:10.1038/nature05392.

Doney, S. C., D. M. Glover, S. J. McCue, and M. Fuentes (2003), Mesoscale variability of Sea-viewing Wide Field-of-view Sensor (SeaWiFS) satellite ocean color: Global patterns and spatial scales, *J. Geophys. Res.*, *108*(C2), 3024, doi:10.1029/2001JC000843.

Draxler, R., and G. D. Hess (2004), Description of the HYSPLIT_4 modeling system, *NOAA Tech. Mem. ERL ARL-224*, Natl. Oceanic and Atmos. Admin, Silver Spring, Md.

Duce, R. A., and N. W. Tindale (1991), Atmospheric transport of iron and its deposition in the ocean, *Limnol. Oceanogr.*, *36*(8), 1715–1726.

Duce, R. A., et al. (1991), The atmospheric input of trace species to the world ocean, *Global Biogeochem. Cycles*, *5*(3), 193–259.

Ekström, M., G. H. McTainsh, and A. Chappell (2004), Australian dust storms: Temporal trends and relationships with synoptic pressure distributions (1960–99), *Int. J. Climatol.*, *24*(12), 1581–1599, doi:10.1002/joc.1072.

Fan, S.-M., W. J. Moxim, and H. Levy, II (2006), Aeolian input of bioavailable iron to the ocean, *Geophys. Res. Lett.*, *33*, L07602, doi:10.1029/2005GL024852.

Frew, R. D., D. A. Hutchins, S. Nodder, S. Sanudo-Wilhelmy, A. Tovar-Sanchez, K. Leblanc, C. E. Hare, and P. W. Boyd (2006), Particulate iron dynamics during FeCycle in subantarctic waters southeast of New Zealand, *Global Biogeochem. Cycles*, *20*, GB1S93, doi:10.1029/2005GB002558.

Gabric, A. J., R. Cropp, G. P. Ayers, G. McTainsh, and R. Braddock (2002), Coupling between cycles of phytoplankton biomass and aerosol optical depth as derived from SeaWiFS time series in the Subantarctic Southern Ocean, *Geophys. Res. Lett.*, *29*(7), 1112, doi:10.1029/2001GL013545.

Gaiero, D. M., J. L. Probst, P. J. Depetris, S. M. Bidart, and L. Leleyter (2003), Iron and other transition metals in Patagonian riverborne and windborne materials: Geochemical control and transport to the southern South Atlantic Ocean, *Geochim. Cosmochim. Acta*, *67*(19), 3603–3623, doi:10.1016/S0016-7037(03)00211-4.

Gaiero, D. M., P. J. Depetris, J. L. Probst, S. M. Bidart, and L. Leleyter (2004), The signature of river- and wind-borne materials exported from Patagonia to the southern latitudes: A view from REEs and implications for paleoclimatic interpretations, *Earth Planet. Sci. Lett.*, *219*(3–4), 357–376, doi:10.1016/S0012-821X(03)00686-1.

Garstang, M., P. D. Tyson, R. Swap, M. Edwards, P. Kallberg, and J. A. Lindesay (1996), Horizontal and vertical transport of air over southern Africa, *J. Geophys. Res.*, *101*(D19), 23,721–23,736.

Gaspari, V., C. Barbante, G. Cozzi, P. Cescon, C. F. Boutron, P. Gabrielli, G. Capodaglio, C. Ferrari, J. R. Petit, and B. Delmonte (2006), Atmospheric iron fluxes over the last deglaciation: Climatic implications, *Geophys. Res. Lett.*, *33*, L03704, doi:10.1029/2005GL024352.

Ginoux, P., M. Chin, I. Tegen, J. M. Prospero, B. Holben, O. Dubovik, and S.-J. Lin (2001), Sources and distributions of dust aerosols simulated with the GOCART model, *J. Geophys. Res.*, *106*(D17), 20,255–20,273.

Gorden, N. D. (1986), Computer-derived air trajectories, *N. Z. Meteorol. Serv. Sci. Rep. 22*, 42 pp., N. Z. Meteorol. Serv., Wellington, New Zealand.

Grini, A., and C. S. Zender (2004), Roles of saltation, sandblasting, and wind speed variability on mineral dust aerosol size distribution during the Puerto Rican Dust Experiment (PRIDE), *J. Geophys. Res.*, *109*, D07202, doi:10.1029/2003JD004233.

Grousset, F. E., P. E. Biscaye, M. Revel, J. R. Petit, K. Pye, S. Joussaume, and J. Jouzel (1992), Antarctic (Dome C) ice-core dust at 18 Ky BP—Isotopic constraints on origins, *Earth Planet. Sci. Lett.*, *111*(1), 175–182, doi:10.1016/0012-821X(92)90177-W.

Gu, Y., W. I. Rose, and G. J. S. Bluth (2003), Retrieval of mass and sizes of particles in sandstorms using two MODIS IR bands: A case study of April 7, 2001 sandstorm in China, *Geophys. Res. Lett.*, *30*(15), 1805, doi:10.1029/2003GL017405.

Hamonou, E., P. Chazette, D. Balis, F. Dulac, X. Schneider, E. Galani, G. Ancellet, and A. Papayannis (1999), Characterization of the vertical structure of Saharan dust export to

the Mediterranean basin, *J. Geophys. Res.*, *104*(D18), 22,257–22,270.
Hand, J. L., N. M. Mahowald, Y. Chen, R. L. Siefert, C. Luo, A. Subramaniam, and I. Fung (2004), Estimates of atmospheric-processed soluble iron from observations and a global mineral aerosol model: Biogeochemical implications, *J. Geophys. Res.*, *109*, D17205, doi:10.1029/2004JD004574.
Healy, T. R. (1970), Dust from Australia—A reappraisal, *Earth Sci. J.*, *4*(2), 106–116.
Holm-Hansen, O., M. Kahru, and C. D. Hewes (2005), Deep chlorophyll a maxima (DCMs) in pelagic Antarctic waters. II. Relation to bathymetric features and dissolved iron concentrations, *Mar. Ecol. Prog. Ser.*, *297*, 71–81, doi:10.3354/meps297071.
Huang, X.-F., J. Z. Yu, L.-Y. He, and Z. Yuan (2006), Water-soluble organic carbon and oxalate in aerosols at a coastal urban site in China: Size distribution characteristics, sources, and formation mechanisms, *J. Geophys. Res.*, *111*, D22212, doi:10.1029/2006JD007408.
Husar, R. B., J. M. Prospero, and L. L. Stowe (1997), Characterization of tropospheric aerosols over the oceans with the NOAA advanced very high resolution radiometer optical thickness operational product, *J. Geophys. Res.*, *102*(D14), 16,889–16,909.
Hutchins, D. A., F. X. Fu, Y. Zhang, M. E. Warner, Y. Feng, K. Portune, P. W. Bernhardt, and M. R. Mulholland (2007), CO_2 control of *Trichodesmium* N_2 fixation, photosynthesis, growth rates, and elemental ratios: Implications for past, present, and future ocean biogeochemistry, *Limnol. Oceanogr.*, *52*(4), 1293–1304.
Jambor, J. L., and J. E. Dutrizac (1998), Occurrence and constitution of natural and synthetic ferrihydrite, a widespread iron oxyhydroxide, *Chem. Rev.*, *98*(7), 2549–2585, doi:10.1021/cr970105t.
Jickells, T. D. (1999), The inputs of dust derived elements to the Sargasso Sea: A synthesis, *Mar. Chem.*, *68*(1–2), 5–14, doi:10.1016/S0304-4203(99)-00061-4.
Jickells, T. D., et al. (2005), Global iron connections between desert dust, ocean biogeochemistry, and climate, *Science*, *308*(5718), 67–71, doi:10.1126/science.1105959.
Johansen, A. M., and J. M. Key (2006), Photoreductive dissolution of ferrihydrite by methanesulfinic acid: Evidence of a direct link between dimethylsulfide and iron-bioavailability, *Geophys. Res. Lett.*, *33*, L14818, doi:10.1029/2006GL026010.
Kiefert, L., G. H. McTainsh, and W. G. Nickling (1996), Sedimentological characteristics of Saharan and Australian dusts, in *Impact of Desert Dust Across the Mediterranean*, edited by S. Guerzoni and R. Chester, pp. 183–190, Kluwer Acad., Amsterdam.
Knight, A. W., G. H. McTainsh, and R. W. Simpson (1995), Sediment loads in an Australian dust storm—Implications for present and past dust processes, *Catena*, *24*(3), 195–213, doi:10.1016/0341-8162(95)00026-O.
Koren, I., Y. J. Kaufman, R. Washington, M. Todd, Y. Rudich, J. V. Martins, and D. Rosenfeld (2007), The Bodele depression: A single spot in the Sahara that provides most of the mineral dust to the Amazon forest, *Environ. Res. Lett.*, *1*(014005), 5 pp., doi:10.1088/1748-9326/1/1/014005.
Krinner, G., and C. Genthon (2003), Tropospheric transport of continental tracers towards Antarctica under varying climatic conditions, *Tellus, Ser. B*, *55*(1), 54–70, doi:10.1034/j.1600-0889.2003.00004.x.
Leys, J., T. Koen, and G. McTainsh (1996), The effect of dry aggregation and percentage clay on sediment flux as measured by a portable field wind tunnel, *Aust. J. Soil Res.*, *34*(6), 849–861, doi:10.1071/SR9960849.
Leys, J., G. McTainsh, C. Strong, S. Heidenreich, and K. Biseaga (2006), DustWatch: Community networks to improve wind erosion monitoring in Australia, paper presented at 6th International Conference on Aeolia Research, Univ. of Guelph, Guelph, Ontario, Canada.
Longhurst, A. (2006), Nutrient limitation: The example of iron, in *Ecological Geography of the Sea*, pp. 71–87, Academic, New York.
Lunt, D. J., and P. J. Valdes (2001), Dust transport to Dome C, Antarctica, at the Last Glacial Maximum and present day, *Geophys. Res. Lett.*, *28*(2), 295–298.
Mackie, D. S., P. W. Boyd, K. A. Hunter, and G. H. McTainsh (2005), Simulating the cloud processing of iron in Australian dust: pH and dust concentration, *Geophys. Res. Lett.*, *32*, L06809, doi:10.1029/2004GL022122.
Mackie, D. S., J. M. Peat, G. H. McTainsh, P. W. Boyd, and K. A. Hunter (2006), Soil abrasion and eolian dust production: Implications for iron partitioning and solubility, *Geochem. Geophys. Geosyst.*, *7*, Q12Q03, doi:10.1029/2006GC001404.
Mahowald, N. M., A. R. Baker, G. Bergametti, N. Brooks, R. A. Duce, T. D. Jickells, N. Kubilay, J. M. Prospero, and I. Tegen (2005), Atmospheric global dust cycle and iron inputs to the ocean, *Global Biogeochem. Cycles*, *19*, GB4025, doi:10.1029/2004GB002402.
Maldonado, M. T., P. W. Boyd, J. LaRoche, R. Strzepek, A. Waite, A. R. Bowie, P. L. Croot, R. D. Frew, and N. M. Price (2001), Iron uptake and physiological response of phytoplankton during a mesoscale Southern Ocean iron enrichment, *Limnol. Oceanogr.*, *46*(7), 1802–1808.
Maring, H., D. L. Savoie, M. A. Izaguirre, L. Custals, and J. S. Reid (2003), Mineral dust aerosol size distribution change during atmospheric transport, *J. Geophys. Res.*, *108*(D19), 8592, doi:10.1029/2002JD002536.
Martin, J. H., R. M. Gordon, and S. E. Fitzwater (1990), Iron in Antarctic waters, *Nature*, *345*(6271), 156–158, doi:10.1038/345156a0.
Matsuki, A., et al. (2005), Morphological and chemical modification of mineral dust: Observational insight into the heterogeneous uptake of acidic gases, *Geophys. Res. Lett.*, *32*, L22806, doi:10.1029/2005GL024176.
McGowan, H. A., G. H. McTainsh, P. Zawar-Reza, and A. P. Sturman (2000), Identifying regional dust transport pathways: Application of kinematic trajectory modelling to a trans-Tasman case, *Earth Surf. Processes Landforms*, *25*(6), 633–647, doi:10.1002/1096-9837(200006)25:6<633:AID-ESP102>3.0.CO;2–J.
McGowan, H. A., B. Kamber, G. H. McTainsh, and S. K. Marx (2005), High resolution provenancing of long travelled dust deposited on the Southern Alps, New Zealand, *Geomorphology*, *69*(1–4), 208–221, doi:10.1016/j.geomorph.2005.01.005.
McTainsh, G. (1985), Dust processes in Australia and West Africa—A comparison, *Search*, *16*(3–4), 104–106.
McTainsh, G. (1998), Dust storm index, in *Sustainable Agriculture: Assessing Australia's Recent Performance*, pp. 55–62, Standing Comm. on Agric. and Resour. Manage., Canberra.
McTainsh, G. (1999), Dust transport and deposition, in *Aeolian Environments, Sediments and Landforms*, edited by A. S. Goudie et al., pp. 181–211, John Wiley, New York.
McTainsh, G., and J. Leys (1993), Soil erosion by wind, in *Land Degradation Processes in Australia*, edited by G. McTainsh and W. C. Boughton, pp. 189–233, Longman Cheshire, Melbourne, Australia.
McTainsh, G., J. Leys, and E. K. Tews (2004), Measuring broadscale dust entrainment and transport in Australia from

meteorological records, paper presented at Wind-blown Dust Workshop, Commonw. Sci. and Ind. Res. Organ., Melbourne, Australia.

McTainsh, G., Y. C. Chan, H. McGowan, J. Leys, and K. Tews (2005), The 23rd October 2002 dust storm in eastern Australia: Characteristics and meteorological conditions, *Atmos. Environ.*, *39*(7), 1227–1236, doi:10.1016/j.atmosenv.2004.10.016.

McTainsh, G., J. Leys, and E. K. Tews (2006), Wind erosion trends for the National State of the Environment Report (2006), Data and methods, in *Australia: State of the Environment Annual Report 2006*, pp. 69–76, Dept. of the Environ. and Water Resour., Canberra.

McTainsh, G. H. (1989), Quaternary aeolian dust processes and sediments in the Australian region, *Quat. Sci. Rev.*, *8*(3), 235–253, doi:10.1016/0277-3791%2889%2990039-5.

McTainsh, G. H., and J. R. Pitblado (1987), Dust storms and related phenomena measured from meteorological records in Australia, *Earth Surf. Processes Landforms*, *12*(4), 415–424, doi:10.1002/esp.3290120407.

McTainsh, G. H., R. Burgess, and J. R. Pitblado (1989), Aridity, drought and dust storms in Australia (1960–84), *J. Arid Environ.*, *16*(1), 11–22.

McTainsh, G. H., A. W. Lynch, and R. C. Burgess (1990), Wind erosion in eastern Australia, *Aust. J. Soil Res.*, *28*(2), 323–339, doi:10.1071/SR9900323.

Meskhidze, N., W. L. Chameides, A. Nenes, and G. Chen (2003), Iron mobilization in mineral dust: Can anthropogenic SO_2 emissions affect ocean productivity?, *Geophys. Res. Lett.*, *30*(21), 2085, doi:10.1029/2003GL018035.

Meskhidze, N., W. L. Chameides, and A. Nenes (2005), Dust and pollution: A recipe for enhanced ocean fertilization?, *J. Geophys. Res.*, *110*, D03301, doi:10.1029/2004JD005082.

Meskhidze, N., A. Nenes, W. L. Chameides, C. Luo, and N. Mahowald (2007), Atlantic Southern Ocean productivity: Fertilization from above or below?, *Global Biogeochem. Cycles*, *21*, GB2006, doi:10.1029/2006GB002711.

Middleton, N. J. (1984), Dust storms in Australia—Frequency, distribution and seasonality, *Search*, *15*(1–2), 46–47.

Miller, R. L., et al. (2006), Mineral dust aerosols in the NASA Goddard Institute for Space Sciences ModelE atmospheric general circulation model, *J. Geophys. Res.*, *111*, D06208, doi:10.1029/2005JD005796.

Mills, M. M., C. Ridame, M. Davey, J. La Roche, and R. J. Geider (2004), Iron and phosphorus co-limit nitrogen fixation in the eastern tropical North Atlantic, *Nature*, *429*(6989), 292–294, doi:10.1038/nature02550.

Perlwitz, J., I. Tegen, and R. L. Miller (2001), Interactive soil dust aerosol model in the GISS GCM 1. Sensitivity of the soil dust cycle to radiative properties of soil dust aerosols, *J. Geophys. Res.*, *106*(D16), 18,167–18,192.

Petit, J. R., et al. (1999), Climate and atmospheric history of the past 420,000 years from the Vostok ice core, Antarctica, *Nature*, *399*(6735), 429–436, doi:10.1038/20859.

Piketh, S. J., P. D. Tyson, and W. Steffen (2000), Aeolian transport from southern Africa and iron fertilization of marine biota in the South Indian Ocean, *S. Afr. J. Sci.*, *96*(5), 244–246.

Piketh, S. J., R. J. Swap, W. Maenhaut, H. J. Annegarn, and P. Formenti (2002), Chemical evidence of long-range atmospheric transport over southern Africa, *J. Geophys. Res.*, *107*(D24), 4817, doi:10.1029/2002JD002056.

Prospero, J. M. (1996), The atmospheric transport of particles to the ocean, in *Particle Flux in the Ocean*, edited by V. Ittekkot et al., pp. 19–52, John Wiley, New York.

Prospero, J. M. (2002), The chemical and physical properties of marine aerosols: An introduction, in *Chemistry of Marine Water and Sediments*, edited by A. Gianguzza et al., pp. 35–85, Springer, Berlin.

Prospero, J. M., and T. N. Carlson (1972), Vertical and areal distribution of Saharan dust over the western equatorial North Atlantic Ocean, *J. Geophys. Res.*, *77*(27), 5255–5265.

Prospero, J. M., R. T. Nees, and M. Uematsu (1987), Deposition rate of particulate and dissolved aluminum derived from Saharan dust in precipitation at Miami, Florida, *J. Geophys. Res.*, *92*(D12), 14,723–14,731.

Prospero, J. M., M. Uematsu, and D. Savoie (1989), Mineral aerosol transport to the Pacific Ocean, in *Chemical Oceanography*, edited by J. P. Riley et al., pp. 187–218, Academic, New York.

Prospero, J. M., P. Ginoux, O. Torres, S. E. Nicholson, and T.E. Gill (2002), Environmental characterization of global sources of atmospheric soil dust identified with the NIMBUS 7 Total Ozone Mapping Spectrometer (TOMS) absorbing aerosol product, *Rev. Geophys.*, *40*(1), 1002, doi:10.1029/2000RG000095.

Rabouille, S., M. Staal, L. J. Stal, and K. Soetaert (2006), Modeling the dynamic regulation of nitrogen fixation in the cyanobacterium *Trichodesmium* sp., *Appl. Environ. Microbiol.*, *72*(5), 3217–3227, doi:10.1128/AEM.72.5.3217-3227.2006.

Raupach, M., G. McTainsh, and J. Leys (1994), Estimates of dust mass in recent major Australian dust storms, *Aust. J. Soil Water Conserv.*, *7*(3), 20–25.

Read, J. F., R. T. Pollard, A. I. Morrison, and C. Symon (1995), On the southerly extent of the Antarctic Circumpolar Current in the southeast Pacific, *Deep Sea Res., Part II*, *42*(4–5), 933–954.

Reid, E. A., J. S. Reid, M. M. Meier, M. R. Dunlap, S. S. Cliff, A. Broumas, K. Perry, and H. Maring (2003), Characterization of African dust transported to Puerto Rico by individual particle and size segregated bulk analysis, *J. Geophys. Res.*, *108*(D19), 8591, doi:10.1029/2002JD002935.

Revel-Rolland, M., P. De Deckker, B. Delmonte, P. P. Hesse, J. W. Magee, I. Basile-Doelsch, F. Grousset, and D. Bosch (2006), Eastern Australia: A possible source of dust in East Antarctica interglacial ice, *Earth Planet. Sci. Lett.*, *249*(1–2), 1–13, doi:10.1016/j.epsl.2006.06.028.

Rosen, J., S. Young, J. Laby, N. Kjome, and J. Gras (2000), Springtime aerosol layers in the free troposphere over Australia: Mildura Aerosol Tropospheric Experiment (MATE 98), *J. Geophys. Res.*, *105*(D14), 17,833–17,842.

Ryan, A. L., and S. R. Cattle (2006), Do sand dunes of the lower Lachlan floodplain contain the same dust that produced parna?, *Aust. J. Soil Res.*, *44*(8), 769–781, doi:10.1071/SR06051.

Sasakawa, M., and M. Uematsu (2005), Relative contribution of chemical composition to acidification of sea fog (stratus) over the northern North Pacific and its marginal seas, *Atmos. Environ.*, *39*(7), 1357–1362, doi:10.1016/j.atmosenv.2004.11.039.

Sedwick, P. N., E. R. Sholkovitz, and T. M. Church (2007), Impact of anthropogenic combustion emissions on the fractional solubility of aerosol iron: Evidence from the Sargasso Sea, *Geochem. Geophys. Geosyst.*, *8*, Q10Q06, doi:10.1029/2007GC001586.

Shao, Y. (2001), A model for mineral dust emission, *J. Geophys. Res.*, *106*(D17), 20,239–20,254.

Shao, Y., J. F. Leys, G. H. McTainsh, and K. Tews (2007), Numerical simulation of the October 2002 dust event in

Australia, *J. Geophys. Res.*, *112*, D08207, doi:10.1029/2006JD007767.

Siefert, R. L., A. M. Johansen, and M. R. Hoffmann (1999), Chemical characterization of ambient aerosol collected during the southwest monsoon and intermonsoon seasons over the Arabian Sea: Labile-Fe(II) and other trace metals, *J. Geophys. Res.*, *104*(D3), 3511–3526.

Spokes, L. J., and T. D. Jickells (1996), Factors controlling the solubility of aerosol trace metals in the atmosphere and on mixing into seawater, *Aquat. Geochem.*, *1*(4), 355–374, doi:10.1007BF00702739.

Spokes, L. J., T. D. Jickells, and B. Lim (1994), Solubilization of aerosol trace metals by cloud processing—A laboratory study, *Geochim. Cosmochim. Acta*, *58*(15), 3281–3287, doi:10.1016/0016-7037(94)90056-6.

Sturman, A. P., P. D. Tyson, and P. C. D'Abreton (1997), A preliminary study of the transport of air from Africa and Australia to New Zealand, *J. R. Soc. N. Z.*, *27*(4), 485–498.

Tagliabue, A., and K. R. Arrigo (2006), Processes governing the supply of iron to phytoplankton in stratified seas, *J. Geophys. Res.*, *111*, C06019, doi:10.1029/2005JC003363.

Takahashi, T., R. A. Feely, R. F. Weiss, R. H. Wanninkhof, D. W. Chipman, S. C. Sutherland, and T. T. Takahashi (1997), Global air-sea flux of CO_2: An estimate based on measurements of sea-air pCO_2 difference, *Proc. Natl. Acad. Sci. U. S. A.*, *94*(16), 8292–8299, doi:10.1073/pnas.94.16.8292.

Tanaka, T. Y., and M. Chiba (2006), A numerical study of the contributions of dust source regions to the global dust budget, *Global Planet. Change*, *52*(1–4), 88–104, doi:10.1016/j.gloplacha.2006.02.002.

Tegen, I., A. A. Lacis, and I. Fung (1996), The influence on climate forcing of mineral aerosols from disturbed soils, *Nature*, *380*(6573), 419–422, doi:10.1038/380419a0.

Tegen, I., S. P. Harrison, K. Kohfeld, I. C. Prentice, M. Coe, and M. Heimann (2002), Impact of vegetation and preferential source areas on global dust aerosol: Results from a model study, *J. Geophys. Res.*, *107*(D21), 4576, doi:10.1029/2001JD000963.

Trenberth, K. E., W. G. Large, and J. G. Olson (1990), The mean annual cycle in global ocean wind stress, *J. Phys. Oceanogr.*, *20*(11), 1742–1760.

Tyson, P. D., and P. C. D'Abreton (1998), Transport and recirculation of aerosols off southern Africa—Macroscale plume structure, *Atmos. Environ.*, *32*(9), 1511–1524, doi:10.1016/S1352-2310(97)00392-0.

Tyson, P. D., M. Garstang, R. Swap, P. Kallberg, and M. Edwards (1996), An air transport climatology for subtropical southern Africa, *Int. J. Climatol.*, *16*(3), 265–291, doi:10.1002/(SICI)1097-0088 (199603)16:3<265:AID-JOC8>3.3.CO;2-D.

VanCuren, R. A., and T. A. Cahill (2002), Asian aerosols in North America: Frequency and concentration of fine dust, *J. Geophys. Res.*, *107*(D24), 4804, doi:10.1029/2002JD002204.

Wagener, T., C. Guieu, R. Losno, S. Bonnet, and N. Mahowald (2008), Revisiting atmospheric dust export to the Southern Hemisphere ocean: Biogeochemical implications, *Global Biogeochem. Cycles*, doi:10.1029/2007GB002984, in press.

Warneck, P. (2003), In-cloud chemistry opens pathway to the formation of oxalic acid in the marine atmosphere, *Atmos. Environ.*, *37*(17), 2423–2427, doi:10.1016/S1352-2310(03)00136-5.

Washington, R., M. Todd, N. J. Middleton, and A. S. Goudie (2003), Dust-storm source areas determined by the total ozone monitoring spectrometer and surface observations, *Ann. Assoc. Am. Geogr.*, *93*(2), 297–313, doi:10.1111/1467-8306.9302003.

Westberry, T. K., and D. A. Siegel (2006), Spatial and temporal distribution of *Trichodesmium* blooms in the world's oceans, *Global Biogeochem. Cycles*, *20*, GB4016, doi:10.1029/2005GB002673.

Westberry, T. K., D. A. Siegel, and A. Subramaniam (2005), An improved bio-optical model for the remote sensing of *Trichodesmium* spp. blooms, *J. Geophys. Res.*, *110*, C06012, doi:10.1029/2004JC002517.

Wolff, E. W., et al. (2006), Southern Ocean sea-ice extent, productivity and iron flux over the past eight glacial cycles, *Nature*, *440*(7083), 491–496, doi:10.1038/nature04614.

World Meteorological Organization (1998), *Manual on Codes: Regional Codes and National Coding Practices*, *WMO Publ. 306*, 318 pp., Geneva.

Xuan, J. (2005), Emission inventory of eight elements, Fe, Al, K, Mg, Mn, Na, Ca and Ti, in dust source region of East Asia, *Atmos. Environ.*, *39*(5), 813–821, doi:10.1016/j.atmosenv.2004.10.029.

Yokoyama, T., and S. Nakashima (2005), Color development of iron oxides during rhyolite weathering over 52,000 years, *Chem. Geol.*, *219*(1–4), 309–320, doi:10.1016/j.chemgeo.2005.03.005.

Young, R. W., et al. (1991), Atmospheric iron inputs and primary productivity: Phytoplankton responses in the North Pacific, *Global Biogeochem. Cycles*, *5*(2), 119–134.

Zender, C. S., H. Bian, and D. Newman (2003), Mineral Dust Entrainment and Deposition (DEAD) model: Description and 1990s dust climatology, *J. Geophys. Res.*, *108*(D14), 4416, doi:10.1029/2002JD002775.

Zhuang, G., Z. Yi, R. A. Duce, and P. R. Brown (1992a), Chemistry of iron in marine aerosols, *Global Biogeochem. Cycles*, *6*(2), 161–173.

Zhuang, G., Z. Yi, R. A. Duce, and P. R. Brown (1992b), Link between iron and sulfur cycles suggested by detection of iron(II) in remote marine aerosols, *Nature*, *355*(6360), 537–539, doi:10.1038/355537a0.

Zuo, Y. G., and J. Zhan (2005), Effects of oxalate on Fe-catalyzed photoxidation of dissolved sulfur dioxide in atmospheric water, *Atmos. Environ.*, *39*(1), 27–37, doi:10.1016/j.atmosenv.2004.09.058.